SCIENTIFIC PAPERS
OF THE UNIVERSITY OF PARDUBICE
Series A
Faculty of Chemical Technology
2 (1996)

$A_2^VB_3^{VI}$ CRYSTALS WITH TETRADYMITE STRUCTURE

Jiří NAVRÁTIL[a], Zdeněk STARÝ[a], Tomáš PLECHÁČEK[a],
Jaromír HORÁK[b] and Petr LOŠŤÁK[c]
[a]Joint Laboratory of Solid State Chemistry
of Academy of Sciences of the Czech Republic and University of Pardubice
[b]Institute of Inorganic Chemistry of Academy of Sciences of the Czech Republic, 160 00 Prague
[c]Department of General and Inorganic Chemistry

Received September 20, 1995

The recent studies of layered thermoelectric materials of A_2B_3 -tetradymite type compounds carried out by JLSSC and Department of Inorganic Chemistry of University of Pardubice are reviewed. The influence of some dopants (III.B - VI.B group) on transport (Seebeck coefficient, Hall constant, electrical conductivity) and optical properties (reflectance and transmittance in IR region) has been observed. From changes of these properties and with the help of quantum-chemical calculations, the view on the point defect nature has been obtained. These results have been applied to polycrystalline materials, too, with regard to the thermoelectric figure of merit.

Introduction

The history of extensive study of A_2B_3 compounds, where A = Bi, Sb and B = Te, Se, is closely connected in particular with the Russian scientist A.F.

Ioffe[1]. He showed in his works that these materials belong among the most promising materials for thermoelectric applications in the medium temperature range. He and his co-workers[2] also proposed that solid solutions of the above-mentioned materials could have better properties from thermoelectric point of view. In sixties many laboratories all over the world studied these materials because of their prospective use in the field of thermoelectricity. Most papers on this subject are reviewed in[3,4]. The majority of these papers dealt with transport properties regarding prospective use of these materials as thermoelectric converters. These compounds turned out to be suitable for studies of relations between structure, bonding and nature of point defects for the following reasons: relatively easy crystal growth at reasonable temperatures, easy sample preparation and particularly high concentration of point defects and their close relation to the structure, electrical and optical properties. This direction has been kept in view in Joint Laboratory of Solid State Chemistry for last ten years. A number of papers were published in close cooperation with Department of General and Inorganic Chemistry, University of Pardubice.

Both the single crystals of Bi_2Te_3, Bi_2Se_3, Sb_2Te_3 and their solid solutions (doped mainly with various impurities of III. - V. B group) have been studied to understand the relations between macroscopic properties and microscopic nature of the crystals (point defects). Recently, the attention has shifted towards the problems which are connected with technological processes in the production of materials for thermoelectric devices. The influence of particle size on the thermoelectric properties was studied to improve the cold-pressed thermoelectric materials.

This paper deals with interpretation of electrical and optical properties (mainly Seebeck coefficient, electrical conductivity, Hall constant, reflectivity and transmittance in IR-region) of the above-mentioned materials. On the basis of the results obtained, possible types of point defects and their interaction are discussed.

This paper presents a review of the most important papers published during the existence of the Joint Laboratory of Solid State Chemistry in cooperation with Department of General and Inorganic Chemistry, University of Pardubice.

Basic Materials

Bi_2Te_3, Bi_2Se_3, Sb_2Te_3 and their solid solutions rank among the family of layered-type semiconductors characterized by the tetradymite structure space group D^5_{3d}. They are marked by distinctive cleavage planes perpendicular to their trigonal c-axis. Their crystal lattice is formed by layers consisting of five atomic planes oriented perpendicularly to the c-axis. Schematically, an arrangement these layers can be expressed like this: ABCAB-CABCA-BCABC. There are weak van der Waals bonds between successive five atomic plane

blocks. Thanks to the bonds these crystals are easy cleavagable along these planes. Lattice parameters of the three basic crystals are presented in Table I.

Table I Lattice parameters of $A_2^VB_3^{VI}$ compounds

Compound	a, Å	c, Å	Ref.
Bi_2Te_3	4.3835	30.487	6
Bi_2Se_3	4.1340	28.546	7
Sb_2Te_3	4.2750	30.490	8

Experimental

Materials Preparation

A modified Bridgman technique was used to prepare the single crystals studied. Polycrystalline ingots were synthesized from the respective elements of 5N purity in evacuated conical quartz ampoules in a horizontal furnace at a temperature of 800-900 °C (depending on the material prepared) for 48 hr. The ampoule containing the polycrystalline material was then suspended into upper hot zone of a Bridgman furnace. After leaving the melt to homogenize at the temperatures of 730 - 800 °C for 24 h, the ampoule was slowly lowered into the temperature gradient, at a rate of 1 - 2 $mm\,h^{-1}$. This technique yielded well cleavable crystals, whose trigonal c-axis was perpendicular to the pulling direction, so that the (0001) plane was parallel to the ampoule axis. The size of the single crystals was approximately 50 mm in length and 10 mm in diameter.

For the studies of the cold pressed materials for the thermoelectric applications the ingots of polycrystalline materials were prepared. After grinding and sieving, the tablets of $2 \times 2 \times 4$ mm^3 size were pressed with the pressure of 2500 MPa and sintered by heating at 510 °C for various times.

Analysis of the Crystals

The single crystals prepared were analyzed by means of KEVEX energy dispersive X-ray measurements. The energy spectra were recorded at the following conditions: accelerating voltage of the primary beam 15 - 20 kV, energy scale divided into 1000 channels (10 eV/channel), detector sensitivity 140 eV, and the detector at an angle of 30° with respect to the sample surface. This method was used for the mixed crystals preferably. To the low concentration of dopants, the atomic absorption spectrometry or extraction photometric method[5] was applied. In some cases the weighed amount of dopant

only was considered.

Determination of Lattice Parameters

The lattice parameters of the single crystals prepared were determined in powder samples by X-ray diffraction analysis using an HZG-4B diffractometer (VEB Freiberger Praezisionsmechanik, GDR). The diffraction maxima were measured by a step procedure using a step of 0.01°. The measurement was carried out in the range of 2θ = 5° - 100° (with Cu $K\alpha$ radiation in the range of 5° - 45°, with Cu $K\alpha_1$ radiation in the range of 45° - 100°). The $K\beta$ radiation was removed by a Ni filter. The calibration of the diffractometer was carried out with polycrystalline Si.

Infrared Region Optical Measurements

The spectral dependence of the reflectance over the range of 4000 - 200 cm^{-1} were measured at room temperature using a Perkin-Elmer Model 684 spectrometer or BIO-RAD FTIR45. The incident beam was nearly perpendicular to the natural cleavage face of the crystal (0001), so that the reflectivity data correspond to the polarization $E \perp c$, where E is the electric field intensity of the electromagnetic radiation.

The transmittance measurements on thin samples whose thickness was of the order of 1 μm were carried out at room temperature using the above- - mentioned spectrophotometers. The radiation was unpolarized but the samples were oriented in such way as to have $E \perp c$.

Measurement of Transport Coefficients

Mainly the Seebeck coefficient, Hall constant and electrical conductivity of the prepared samples were measured. A thermoelectric figure of merit of polycrystalline and cold-pressed samples was also measured.

For the conductivity measurements, samples of 15 × 3 × (0.1 – 0.3) mm^3 dimensions were cut from the natural cleavage faces of the crystals. The values of the electrical conductivity σ were calculated from the measured voltage drop across two contacts on the sample, passed by alternating current at a frequency of 170 Hz and intensity 50 mA. Owing to the fact that the current passed in the direction perpendicular to the trigonal axis c, the values $\sigma_{\perp c}$ were determined in this way. The measurements were mostly carried out over the temperature range from 100 to 420 K.

The Hall coefficient was measured in the same samples, at the same time and over the same temperature range as the electrical conductivity. The AC

technique at a frequency of 170 Hz in the $\mathbf{B}\|c$ orientation with the value of **B** equal to $1.1\,T$ was used.

The Seebeck coefficient was determined for the direction $\Delta T \perp c$, temperature gradient on the sample not exceeding 10 K.

The figure of merit Z in the polycrystalline or cold-pressed samples was measured by means of modified Harman method which started from the equation for stable heat flow in the sample

$$SIT = \lambda \Delta T \tag{1}$$

where S is the Seebeck coefficient, I is the electrical current, T is the temperature of cold junction of sample, λ is the thermal conductivity and ΔT is the temperature difference in the sample. The equation (1) is valid for the case of the small electrical current and, consequently, small heat exchange with the surroundings. The figure of merit was calculated from the equation

$$Z = \frac{U_{-} - U_{\sim}}{U_{\sim} T} \tag{2}$$

where $U_{\sim} = RI$, $U_{-} = RI + S\Delta T$ and ΔT is taken from Eq. (1)

Calculation of the Bonding Character in the Crystals

In order to be able to evaluate the relations between the concentration of AS defects and the changes in bonding conditions as a function of content of some dopants, we carried out a quantum-chemical calculation of the bonding conditions using the computer program TOPOLOGY[12]. The quantum-chemical procedure is merely a version of HMO method extended on the basis of all valence orbitals. The calculation is performed in the basis of equivalent orbitals, and the interactions of all equivalent orbitals between the nearest neighbours are taken into account. The Coulomb integrals were identified with the scaled orbital electronegativities and the resonace integrals were calibrated on a set of homonuclear diatomics. The details of the method and the calibrations can be found in[13].

The calculation was carried out for a section of the crystal layer between the van der Waals gaps. This section was formed by 31 atoms that had altogether 174 valence orbitals. The arrangement of the crystal section used in the calculation is represented in Fig. 1. For clarity, only three atomic layers are depicted, the Te^1, Sb and Te^2 layers.

Notions Definitions

1. Polarity of the bond c between atoms A and B is defined as the difference in the electron density on the orbitals in the direction of bond c on atoms

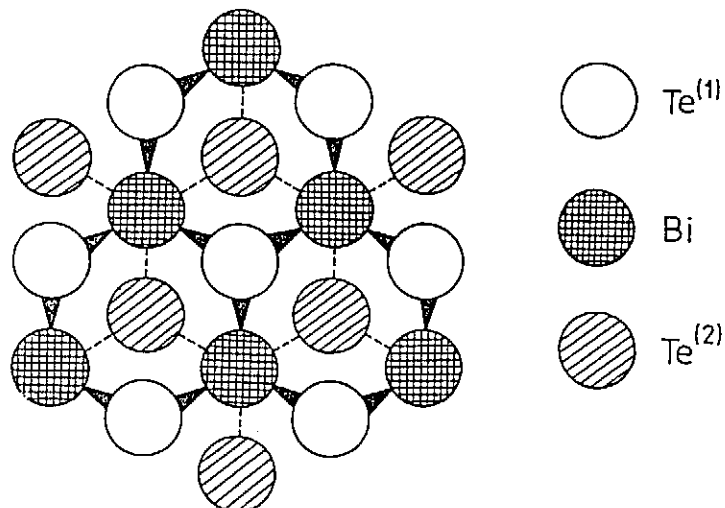

Fig. 1 A part of the crystal section use dfor calculation. The bond are drawn relative to the Bi atomic plane

A and B. It is given in units of the elementary charge and denoted with p.

2. Electron density between the stacks is the density of electrons on the orbitals pointing to the van der Waals gap. It is given in units of the elementary charge and referred to one atom. Its symbol is ρ_g.
3. Electron density in the layers is also referred to one atom and given in units of the elementary charge. The corresponding symbol is ρ_l.
4. Bond order expresses the bond multiplicity (corresponds to the electron density in the space of the bond). It is a dimensionless quantity and is denoted by BO.

Discussion

The Influence of III. B Group Dopants (Ga, In) on the Properties of the Basic Materials

The highest solubility of the group IIIb chalcogenides has been observed in the Sb_2Te_3-In_2Te_3 system, as well as in the Bi_2Se_3-In_2Se_3 and Bi_2Te_3-In_2Te_3 systems[6,7]. The solubility of thallium chalcogenides is markedly lower in chalcogenides with a tetradymite structure[8]. The lowest solubility has been found in the system containing gallium chalcogenides. In the below-mentioned papers, attention was paid to mixed crystals with indium chalcogenides mainly.

$Sb_{2-x}In_xTe_3$ System

The reflectance spectra of $Sb_{2-x}In_xTe_3$ samples are presented in Fig. 2. These were interpreted using the relations for the real and imaginary parts of the complex dielectric function following from the Drude-Zener theory[9]

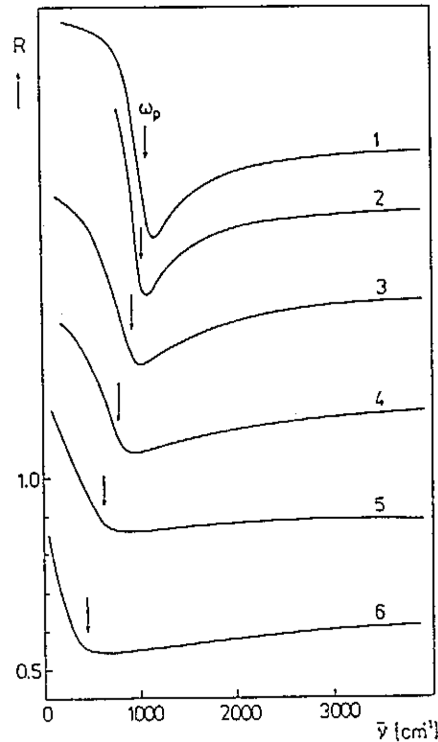

Fig. 2 Reflectance spectra of $Sb_{2-x}In_xTe_3$ samples. The curves are denoted according to Table II

$$\varepsilon_1 = n^2 - k^2 = \varepsilon_\infty\left(1 - \frac{1}{(\omega/\omega_p)^2 + (1/\omega_p\tau)^2}\right) \tag{3}$$

$$\varepsilon_2 = 2nk = \frac{\varepsilon_\infty}{\omega\tau}\,\frac{1}{\omega\tau(\omega/\omega_p)^2 + (1/\omega_p\tau)^2} \tag{4}$$

where n is the index of refraction, k is the index of extinction, τ is the optical relaxation time, ε_∞ the high frequency dielectric constant and ω_p the plasma frequency, which is given for one kind of free carriers by

$$\omega_p = \left(\frac{Ne^2}{\varepsilon_0 \varepsilon_\infty m^*{\perp}}\right)^{1/2} .$$

In this formula, $m^*{\perp}$ is the free carrier effective mass in the direction perpendicular to the trigonal axis c, N the carrier concentration, ε_0 the permittivity of the free space and e the electron charge. The calculation was performed using the formula

$$R = \frac{(n-1)^2 + k^2}{(n+1)^2 + k^2} \tag{6}$$

The results of optical and transport measurements are contained in Table II. In agreement with Ref.[10] the valence band of Sb_2Te_3 is described with nonparabolic six valley model from which follows the structure coefficient $\gamma = 0.77$ in the expression for the Hall constant $R_H = r\gamma/(eP)$. This value was used for the determination of free carrier concentration (r value was considered as one).

Table II Transport coefficients, plasma resonance frequence and optical relaxation time of $Sb_{2-x}In_xTe_3$ samples

	1	2	3	4	5	6
x	0.0	0.050	0.098	0.220	0.29	0.41
$R_H(B\parallel c)$ $cm^3\,A^{-1}\,s^{-1}$	0.058	0.067	0.090	0.148	0.240	0.190
$P/\gamma A \times 10^{-19}$ cm^{-3}	10.78	9.33	6.94	4.22	2.60	3.29
$S \perp c$ $\mu V\,K^{-1}$	74	80	85	114	172	215
$\omega_p(E\perp c)\times 10^{-14}$ s^{-1}	1.95	1.86	1.7	1.26	1.19	0.82
$(P/m^*{\perp})\times 10^{-20}$ cm^{-3}	5.85	5.33	4.36	2.34	2.00	0.94
$\tau_{opt}\times 10^{14}$ s	2.5	2.4	1.8	0.95	0.82	0.84

According to the results of Ref.[11], undoped Sb_2Te_3 crystals exhibit a pronounced superstoichiometric content of Sb atoms (approx. 8×10^{19} cm^{-3}) that are built into the Te sublattice and thus form antisite (AS) defects Sb_{Te}-type. The charge in these defects is compensated by holes. The results of the measurements of the Hall coefficient and the values of plasma resonance frequency obtained in a series of $Sb_{2-x}In_xTe_3$ crystals show that increasing content of the built-in In

atoms leads to a decrease in the free carrier concentration. In agreement with this finding, the Seebeck coefficient increases with x and the value of the Fermi level decreases. Hence, it has been shown by independent methods that the built-in indium atoms lower the concentration of the holes. The incorporation of In atoms into the Sb_2Te_3 can be realized in several ways:

(a) In atoms enter as interstitials within the structural layers;
(b) In atoms occupy positions in the Sb sublattice;
(c) In atoms occupy Te^2 sites in the Te sublattice with octahedral coordination to the Sb atoms;
(d) In atoms occupy Te^1 sites in the Te sublattice;
(e) In atoms enter the van der Waals gaps in the layered structure of Sb_2Te_3.

According to the results obtained we can excluded cases (a) and (e), because both defects would lead to the creation of free electrons, i.e. to a very strong decrease in the hole concentration. Also the formation of In_{Sb}'' defects created by the incorporation of In atoms in the Sb sublattice (b) is impossible owing to the electron configuration of In and Sb atoms. Such a process would lead to an increase in the hole concentration. This is in contradiction with the experiment. Even the substitutional defect In atom in the Te sublattice (c, d) would cause a negatively charged defect and so lead to an increase in the hole concentration, which is contrary to the experiment. Therefore, we accept the following process for the incorporation of In atoms in the Sb_2Te_3 lattice.

The In atoms introduced into the Sb_2Te_3 crystal form uncharged substitutional defects in the Sb sublattice; their formation can be described as follows

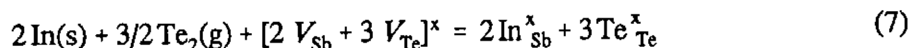

$$2\,In(s) + 3/2\,Te_2(g) + [2\,V_{Sb} + 3\,V_{Te}]^x = 2\,In_{Sb}^x + 3\,Te_{Te}^x \qquad (7)$$

where $[2V_{Sb} + 3V_{Te}]^x$ represents the increase in the crystal volume and In_{Sb}^x is an uncharged substitutional defect. The change in the electron configuration of the In atoms forming the In_{Sb}^x point defects can be expressed symbolically as $In(5s^2\,5p^1) \rightarrow In_{Sb}(5s^0\,5p^3)$.

Accepting this assumption, we may explain the decrease in the number of AS defects Sb'_{Te}-type in the following way: introduction of In atoms into the Sb sublattice gives rise to formally uncharged In_{Sb}^x defects. In Table III, the scaled orbital electronegativities of Sb, Te and In atoms for s, p and d orbitals are entered. The value of the scaled electronegativity for the $sp^3\,d^2$ orbital is given in the form of the diagonal term of H-core matrix. It is evident from these values that indium is more electropositive than antimony, so that one can expect the In_{Sb}^x defect to acquire a partial positive charge. The assumed changes in the bonding conditions in the crystal lead to an increase in ionicity; a larger ionicity suppresses the probability of the transition of a positively polarized particle into the sublattice of negatively polarized particles, leading thus to a decrease in the concentration of AS defects.

The above-mentioned qualitative idea of the changes in bonding

Table III Diagonal members of H core matrix (scaled electronegativity)

Atom	Orbital			
	s	p	d	$sp^3 d^2$
Sb	1.245	0.669	0.132	0.7702
Te	1.409	0.772	0.167	0.7883
In	0.926	0.479	0.072	0.7366

parameters is supported by a quantum chemical calculation which permits us to calculate the changes in the electron density in the atomic layers. Figure 3 shows the change in the electron density on the individual layers of the $Sb_{2-x}In_xTe_3$ crystal (for x = 0.0 - 0.66). As it is evident from the figure the charge corresponding to the antimony sublattice becomes markedly more positive and the electron density on the outer atomic layers Te^1 increases. Also the Te^2 layers acquire a higher electron density. The polarity of the bonds between the atoms of individual layers (see Table IV) was determined for the calculated data of electron distribution.

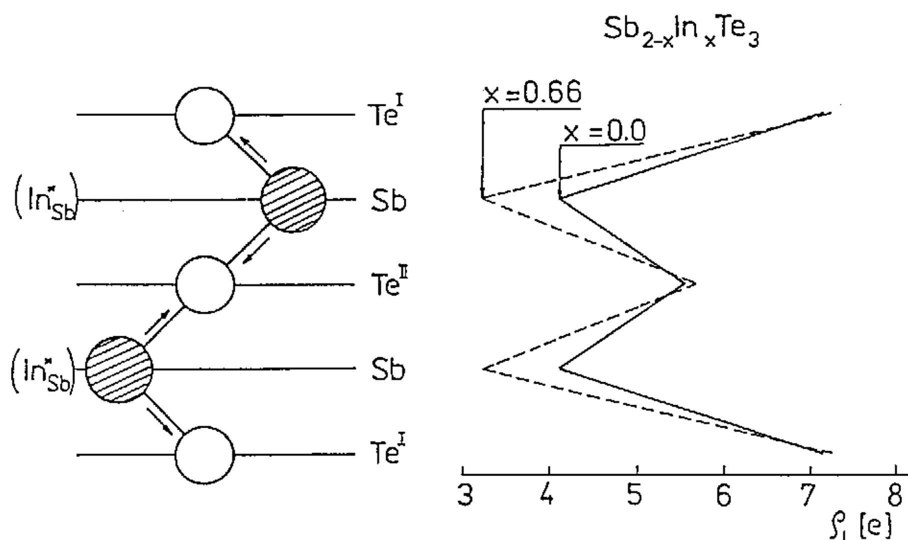

Fig. 3 Electron density along the cross-section of one crystal layer (solid line - Sb_2Te_3, dashed line $Sb_{1.34}In_{0.66}Te_3$

The results of quantum-chemical calculations show unambiguously that the In atoms introduced into the Sb sublattice bring about an increase in the average bond ionicity. The results of the papers[14-17] imply that increasing ionicity

of the crystal leads to a decrease in the probability of the formation of AS defects.

The concentration of AS defects in undoped crystal can be expressed by the equation

$$N_{AS} = k_1 \exp\left(-\frac{E_0}{k_B T_M}\right) \tag{8}$$

where k_1 is the characteristic constant for given crystal, E_0 is the formation energy of the AS defects, k_B the Boltzmann constant and T_M the temperature of melting. The introduction of foreign atoms that alter the bond polarity results in a change in the energy of formation of AS defects. In doped or mixed crystals the energy of formation of the AS defects is given by the sum $E_0 + \Delta E$, where ΔE is the polarization energy.

Table IV Some data obtained by the program TOPOLOGY for $Sb_{2-x}In_xTe_3$ system

$Sb_{2-x}In_xTe_3$	Bond polarity* p, e		Electron density inside the gap ρ_g, e	Bond order BO	
x	I	II		I	II
0.000	0.404	0.226	3.904	0.521	0.665
0.165	0.453	0.268	3.910	0.520	0.675
0.330	0.492	0.307	3.912	0.522	0.683
0.495	0.536	0.353	3.915	0.523	0.685
0.660	0.579	0.400	3.918	0.526	0.687

$Sb_{2-x}In_xTe_3$	Electron density inside the layers** ρ_l, e		
x	I	II	III
0.000	7.130	4.105	5.542
0.165	7.160	3.884	5.593
0.330	7.180	3.672	5.612
0.495	7.207	3.440	5.637
0.660	7.234	3.211	5.666

* I Te^1 - Sb(In), II Te^2 - Sb(In)
** I Te^1, II Sb(In), III Te^2

In the case of $Sb_{2-x}In_xTe_3$ mixed crystals E_0 = 0.35 eV at x = 0, according to Ref.[15]; the polarization energy ΔE will increase with increasing concentration of In atoms because In is more electropositive then Sb. Fig. 4

shows the dependence of $E_0+\Delta E$ on the concentration of the In atoms in the lattice. In calculating ΔE we adopted the assumption that only one type of charged defect exists in the mixed crystal lattice, i.e., the AS defects in the sense of In_{Sb}. Therefore, the concentration of the AS defects is equal to the concentration of holes and we can determine ΔE from the equation

$$\frac{N'_{AS}}{N_{AS}} = \frac{\gamma(x)r(x)R_H(0)}{\gamma(0)r(0)R_H(x)} = \exp\left(\frac{-\Delta E}{k_B T_M}\right) \tag{9}$$

where γ is the structure factor and r is the Hall factor. The results of ΔE calculation are presented in Fig. 4.

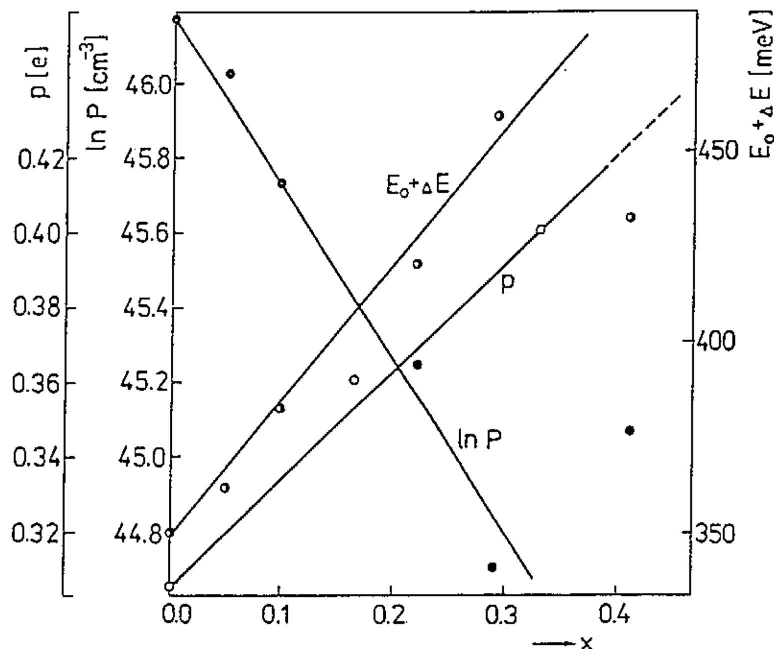

Fig. 4 Dependence of average bond polarity, free carrier concentration and energy of formation of the antisite defect on the composition of $Sb_{2-x}In_xTe_3$ crystals

The formation of AS defects is a consequence of the very weak polarity of the bonds between the atoms in the crystal lattice. If, by introducing suitable impurity atoms, we provoke an increase in bond polarity, the energy of formation of AS defects increases and their concentration decreases; conversely, by suppressing the bond polarity - which is rather low in Sb_2Te_3 crystals - we create the conditions favourable to the formation of AS defects. This qualitative view of relations between the concentration of the AS defects and bond polarity is supported by quantum-chemical calculation.

In our opinion, the idea of relation between the concentration of AS defects and the bond polarity has general validity and can also be applied to

other crystals containing AS defects. The above-mentioned ideas are described in more detail in Ref.[18].

$Bi_{2-x}In_xTe_3$ System

The growth of these crystals, their structure, and some physical properties characterizing their semiconducting nature were described in Ref.[6]. More recent studies on the variation of the free carrier concentration with indium content have been reported in Refs[14,15]. Up to the concentration $x = 0.1$, the $Bi_{2-x}In_xTe_3$ mixed crystals exhibit hole conductivity, for $x > 0.1$ the majority carriers are electrons. The variations of the hole concentration in dependence on the content of In atoms have been qualitatively explained in Ref.[15] on the assumption that the incorporation of In atoms into the crystal lattice results in their interaction with AS defects of Bi'_{Te}-type. The interaction leads to uncharged In^{x}_{Bi} defects, hence to a decrease in the concentration of holes. The disappearance of AS defects is thus accompanied by the suppression of the hole concentration. Further increase in the content of In atoms in the lattice results in crystals of n-type conductivity.

The concentration of In(x) in the mixed crystals, the electrical conductivity, and the Hall constant are summarized in Table V. From the Hall constant the concentration of the holes P was determined using the formula $R_H = r\gamma/(eP)$ (see meanings of terms above). The value of $\gamma = 0.514$ for undoped Bi_2Te_3 crystals was determined by Brebrick[19]. Since the $Bi_{2-x}In_xTe_3$ samples do not exhibit large differences in the concentration of free carriers and since the band structure of $Bi_{2-x}In_xTe_3$ mixed crystals is not yet known, we take the value of γ as constant. The Hall factor r is taken equal to unity.

As it follows from the results of measurements of the electrical conductivity and the Hall constants, an increasing number of In atoms built into the Bi_2Te_3 crystal lattice results in a slight decrease in the concentration of free carriers (see Fig. 5). This finding is in accordance with the results of paper[6]. These authors, trying to account for this phenomenon, suppose that indium atoms are incorporated both into the Bi and into the Te-sublattice, with Te atoms entering also the Bi-sublattice at the same time. Such an explanation seems to be rather complicated and is hardly acceptable. The existence of interstitials of In atoms does not appear probable either - it would lead to a drastic decrease in the concentration of holes. The experiment, however, shows that the incorporation of larger number of In atoms into the lattice of the mixed crystal leads to a relatively small decrease in the free carrier concentration. The formation of substutional In''_{Bi} or In'_{Bi} defects carrying negative charge, which should be expected in view of the electronic configuration of Bi and In atoms, is unacceptable, too, as these defects would increase the concentration of holes. Therefore a relatively small decrease in the hole concentration can be explained in the similar way as in the case of $Sb_{2-x}In_xTe_3$ mixed crystals: the In atoms

enter the sites in the Bi-sublattice and form uncharged In^{x}_{Bi} defects. This process can be qualitatively described by the equation

$$(2\,V_{Bi} + 3\,V_{Te})^{x} + 2\,In + 3/2\,Te_2 = 2\,In^{x}_{Bi} + 3\,Te^{x}_{Te} \quad . \qquad (10)$$

Table V Transport coefficients and energy of formation of anti-site defects in $Bi_{2-x}In_xTe_3$ crystals

Composition	$\sigma_{\perp c}$	$R_H\,(B \parallel c)$	$R_H\sigma$	$E + \Delta E$	ΔE
x	$\Omega^{-1}\,cm^{-1}$	$cm^3\,A^{-1}\,s^{-1}$	$cm^2\,V^{-1}\,s^{-1}$	eV	meV
0.000	660	0.44	290	0.500	0
0.015	537	0.54	290	0.515	15
0.040	335	0.77	258	0.541	41
0.045	245	0.81	232	0.545	45

Uncharged In^{x}_{Bi} defects are then positively polarized due to the higher electropositivity of In compared to Bi. In the sense of the above-mentioned ideas one can qualitatively formulate the influence of In defects on the concentration of AS defects in the following way: increasing bond polarity (see Table VI) with increasing concentration of In atoms results in a decrease in the probability of formation of AS defects and thus a decrease in hole concentration. The explanation is the same as that for the $Sb_{2-x}In_xTe_3$. However, the concentration of holes is much lower in the $Bi_{2-x}In_xTe_3$. It is possible to change the type of conductivity by addition of higher content of indium. It seems that, besides the AS defects Bi'_{Te}, the considerable concentration of vacancies $V^{\bullet}_{Te}$ exists in Bi_2Te_3 (Ref.[20]).

The energy of formation of AS defects in $Bi_{2-x}In_xTe_3$ samples for $x = 0$ to 0.05 was determined from the data on the concentration of AS defects in these mixed crystals using the Eq. 8. The results, shown in Fig. 6 corroborate the qualitative ideas leading to the conclusion that the probability of the formation an AS defects is lower in crystals with higher bond polarity.

The qualitative picture that the formation of uncharged In^{x}_{Bi} defects affects the bond polarity is also confirmed by a quantum-chemical calculation. The variations of the bond polarity in dependence of the concentration of In atoms are presented in Table VI. It follows from Table VI that the p value is proportional to the concentration x of In atoms built into the crystal lattice.

It is of interest to compare the concentration of AS defects in the Sb_2Te_3 and the Bi_2Te_3 crystals prepared from stoichiometric melts, and also the influence of In atoms on the concentration of AS defects. The higher bond polarities of $Bi-Te^1$ or $Bi-Te^2$ bonds than the corresponding values of $Sb-Te^1$ or $Sb-Te^2$ bonds are responsible for the fact that the concentration of AS

defects is lower in Bi_2Te_3 than in Sb_2Te_3 - approximately 1×10^{19} cm^{-3} (according to Ref.[11]) as compared with 8×10^{19} cm^{-3} in undoped Sb_2Te_3. An identical concentration of In atoms built into the lattice of both tellurides will thus result in larger variations of the concentration of AS defects in Sb_2Te_3 than in Bi_2Te_3, but in view of a lower concentration of AS defects in Bi_2Te_3, a smaller concentration of In atoms built into the lattice of Bi_2Te_3 will be sufficient to suppress the concentration of AS defects. While the indium

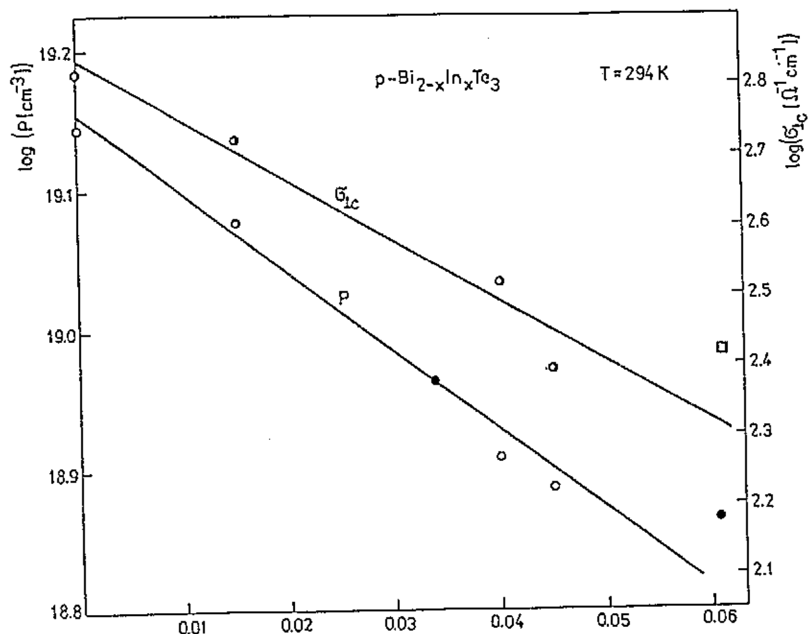

Fig. 5 Semilogarithmic plot of electrical conductivity and hole concentration vs. composition (T = 294 K, ● Rosenberg and Strauss[6])

Table VI Some data obtained by the program TOPOLOGY for $Bi_{2-x}In_xTe_3$ system

$Bi_{2-x}In_xTe_3$	Bond polarity* p, e		Electron density inside the gap ρ_g, e	Bond order BO	
x	I	II		I	II
0.000	0.573	0.372	4.043	0.604	0.467
0.165	0.603	0.403	4.039	0.610	0.474
0.330	0.624	0.437	4.036	0.619	0.480
0.495	0.648	0.471	4.029	0.626	0.479
0.660	0.678	0.510	4.033	0.629	0.479

Table VI Continued

$Bi_{2-x}In_xTe_3$	Electron density inside the layers** ρ_l, e		
x	I	II	III
0.000	7.510	3.637	6.019
0.165	7.512	3.462	6.021
0.330	7.509	3.299	6.024
0.495	7.502	3.125	6.030
0.660	7.518	2.940	6.040

* I Te^1 - Bi(In), II Te^2 - Bi(In)
** I Te^1, II Bi(In), III Te^2

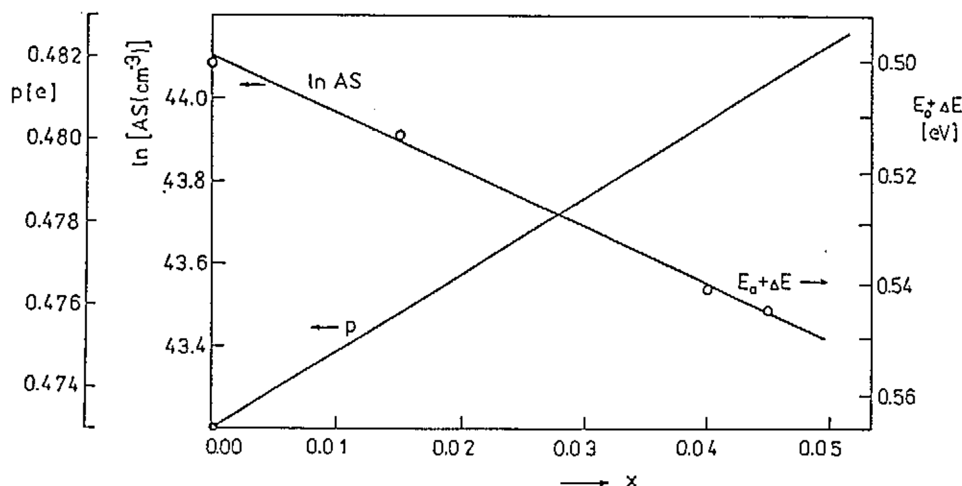

Fig. 6 Correlation among the energy of polarization ΔE, energy of formation of anti-site defects E_0 and concentration of anti-site defects. A part of the calculated polarity as a function of composition is also plotted for information

concentration corresponding to x = 0.10 in $Bi_{2-x}In_xTe_3$ crystals leads to complete suppression of AS defects and to the onset of n-type conductivity[6], the same concentration of In atoms built into Sb_2Te_3 lattice is not sufficient to suppress the concentration of AS defects fully and to give rise to n-type conductivity, although it results in a larger decrease of the concentration of holes.

Introduction of a relatively small amount of In (10^{18} atoms In cm^{-3}) into the Bi_2Se_3 crystals leads to not easily measurable changes in the transport coefficients. On incorporating a larger quantity of In atoms (up to the concentration of $x = 0.15$) into the $Bi_{2-x}In_xSe_3$ lattice an increase of the free carrier concentration was observed. If $x > 0.15$, the $N = f(x)$ dependence passes through a maximum and the electron concentration decreases.

In order to evaluate the observed behaviour, it is necessary to show what point defects arise on incorporation of In atoms into the Bi_2Se_3 lattice, or how the built-in In interacts with the defects in the Bi_2Se_3 lattice. The In atoms can enter the Bi_2Se_3 lattice in one or more of the following ways:

(a) In atoms occupy positions in the Bi sublattice; in view of the electron configuration of In atoms these can form substitutional defects carrying a negative charge (In''_{Bi} or In'_{Bi});
(b) In atoms form interstitial defects carrying a positive charge;
(c) In atoms can enter the van der Waals gap;
(d) In atoms can occupy Se sublattice sites.

The defects quoted in (a) would give rise to a steep decrease in the free electron concentration which is in contradiction to experiment. The defects quoted in (b) also seem to be unrealistic: their existence would has to lead to a steep increase in the free electron concentration. A comparison of the concentration of the built-in In atoms with the rise in the free electron concentration excludes the existence of interstitial defects. The defects quoted in (c) do not seem to be probable. If in the course of such a process In atoms became ionized, the free-electron concentration would increase much more rapidly than this one experimentally observed.

Therefore the apparently anomalous increase and subsequent decrease of the free electron concentration with increasing In content can be explained in the following way: In atoms occupy the Bi sublattice sites and form uncharged defects. This process conforms with the ideas brought up by Krebs[21] and can be explained similarly as in the case of indium incorporation into Bi_2Te_3 lattice by the equation

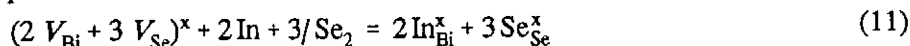

$$(2\,V_{Bi} + 3\,V_{Se})^{x} + 2\,In + 3/Se_2 = 2\,In^{x}_{Bi} + 3\,Se^{x}_{Se} \quad (11)$$

The above-mentioned formulation of uncharged defects is necessarily connected with the idea that the electrons are carried over from 5s orbitals to 5p orbitals[21]. Adopting the idea about the formation of positively polarized In^{x}_{Bi} defects, one can account for the variations in the electron concentration (as shown in Fig. 8 in the form of $N/m_{\perp}$) on the basis of the following concept.

Beside anion vacancies $V^{\bullet}_{Se}$ in Bi_2Se_3 crystals there also exist AS defects of Bi'_{Se}. This assumption is not unrealistic: the bonds between Bi and Se atoms are little polarized and ionicity fraction is low. On the basis of ideas formulated

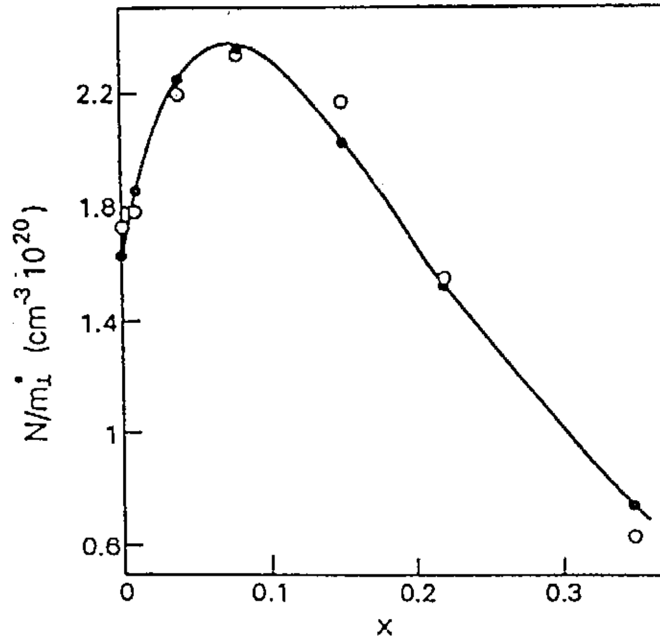

Fig. 8 The dependence of $N/m_\perp^*$ on the indium concentration (full circles - calculation, empty circles - experiment)

in Refs[15,18,22] and above, there is no reason why not to admit the existence of anionic AS defects in the Bi_2Se_3 lattice. The incorporation of indium atoms results in an increase of the polarity of the $In_{Bi}^{x\,\delta+}-Se^{(1)}$ and $In_{Bi}^{x\,\delta+}-\ e^{(2)}$ bonds, thus increasing the mixed-crystal ionicity and decreasing the probability of the formation of AS defetcs. It is possible to describe the decrease in the concentration of AS defects by means of the relation

$$N_{AS} = kN_0 \exp\left(-\frac{E_0 + \Delta E}{k_B T_M}\right) \tag{12}$$

where N_{AS} denotes the concentration of AS defects, E_0 the energy required to form one AS defect, k_B the Boltzmann constant and T_M the melting point of the crystal. ΔE, the so-called "polarization" energy is a contribution to the energy of formation of AS defects. This equation is similar to Eq. (8), where $k_1 = kN_0$ that means the concentration of AS defects in hypotetic covalent Bi_2Se_3. With rising polarity of the crystals (see Table VII), due to the incorporation of indium into the cation sublattice, the concentration of AS defects of Bi_{Se}'-type should drop. This effect is responsible for the initial increase of the free-electron concentration since it lowers the production of holes with which the free electrons recombine. The decrease in the free-carrier concentration observed in the range of higher indium content built into the

lattice is probably due to a lowering of the concentration of $V_{Se}^{\cdot}$ vacancies in $Bi_{2-x}In_xSe_3$ crystal lattice. This lowering of the concentration of $V_{Se}^{\cdot}$ with increasing In content is connected to the fact that the increasing concentration of In atoms in the mixed crystal leads to an increase in the gap width due to higher crystal ionicity. In isostructural $Bi_{2-x}In_xSe_3$ crystals this is manifested, among others, by a decrease of the mobility of the free carriers. Increasing ionicity of $Bi_{2-x}In_xSe_3$ crystals with increasing In content obviously leads to a lowering of the departure from stoichiometry and hence to a decrease in the concentration of vacancies. This in turn brings about a decrease in the free-electron concentration, as shown by experiments (see Figs 7 and 9). The diminishing departure from stoichiometry with increasing crystal ionicity shows - as seen from the variation of the drop of the free-carrier concentration with increasing x - an exponential behaviour.

The observed decrease in the free electron concentration and thus also in the concentration of $V_{Se}^{\cdot}$ defects is in good agreement with the ideas brought up by van Vechten[23]. This author states that in the crystal lattice of binary compounds the vacancies are more numerous for the atoms of small radii. Thus, in a series of isostructure crystals, one can expect an increase in the concentration of vacancies with increasing difference between the sizes of cations and anions. In $Bi_{2-x}In_xSe_3$ crystals the larger Bi atoms are substituted by smaller In atoms, the "effective" atom radius in the cation sublattice decreases, which results in a decrease in the difference between the sizes of the atoms in cationic and anionic sublattices. This is manifested by a decrease in the concentration of selenium vacancies $V_{Se}^{\cdot}$. A simple quantitative analysis of the above-mentioned phenomenon is described in more detail in Ref.[24].

Table VII Some data obtained by the program TOPOLOGY for $Bi_{2-x}In_xSe_3$ system

$Bi_{2-x}In_xSe_3$	Bond polarity* p, e		Electron density inside the gap ρ_g, e	Bond order BO	
x	I	II		I	II
0.000	0.548	0.353	4.012	0.618	0.481
0.165	0.575	0.382	4.015	0.631	0.490
0.330	0.606	0.420	4.014	0.639	0.489
0.495	0.630	0.454	4.008	0.646	0.488
0.660	0.659	0.492	4.011	0.648	0.487

Table VII Continued

$Bi_{2-x}In_xSe_3$	Electron density inside the layers** ρ_l, e		
x	I	II	III
0.000	7.438	3.694	5.939
0.165	7.442	3.527	5.941
0.330	7.457	3.351	5.969
0.495	7.449	3.178	5.974
0.660	7.466	2.995	5.986

* I Se^1 - Bi(In), II Se^2 - Bi(In)

** I Se^1, II Bi(In), III Se^2

Lattice Parameters and As Defects

The validity of "polarization" model can be supported by measuring of lattice parameters. In Figs 10, 11, 12 dependences of lattice parameters a and c on the In content are shown. While a-parameter decreases with increasing In content in all the systems studied, c-parameter exhibits a maximum for both $Bi_{2-x}In_xSe_3$ and $Sb_{2-x}In_xSe_3$. Also for $Bi_{2-x}In_xTe_3$ there is a small maximum in $c = f(x)$ dependence, but it is shifted towards lower In content.

As it can be seen from the foregoing text the In incorporation into the crystal lattice leads to suppression of AS concentration. With regard to the fact that the concentration of smaller atoms in the lattice increases, one could expect (according Vegard's rule) a monotonous decrease in all lattice parameters. Initial rise of c-parameter can be explained as follows: indium entering into the lattice suppresses the AS defect concentration and thus allows the bigger anion atoms to enter their original position. The concentration of cation atoms in anion sublattice decreases. Supposing the "polarization" model is valid, one can expect that the most distinct maximum of $c = f(x)$ dependence will appear in the system with biggest AS defect concentration and vice versa, and will be shifted to bigger In concentration. Comparison of Figs 10, 11, 12 supports this idea.

The a-parameter does not exhibit any maximum, but its drop is at first very slow with increasing In content. This fact is probably caused by lower flexibility of lattice in the direction parallel to the cleavage planes. In this direction we move along hexagonal close packed atomic planes.

Apparently incomparable quantities are summarized in Table VIII. As it can be seen from the table, the close correlation of these quantities also supports the validity of the "polarization" model.

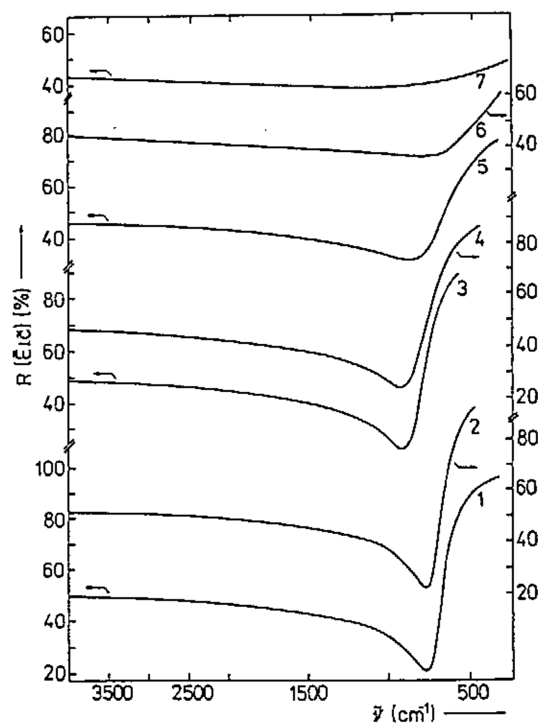

Fig. 7 Reflectance spectra of $Bi_{2-x}In_xSe_3$ samples: 1 - x = 0, 2 - x = 0.01, 3 - x = 0.08, 4 - x = 0.15, 5 - x = 0.22, 6 - x = 0.34, 7 - x = 0.45

Table VIII Values of bond polarity, AS defects formation energy, AS defects concentration and location of maximum of lattice parameter c

Crystal	Bond polarity		E_0 eV	AS 10^{19} cm^{-3}	$x_{c\text{-max}}$*
	p_1	p_2			
Sb_2Te_3	0.4040	0.2265	0.35	8.14	0.250
Bi_2Se_3	0.5477	0.3527	0.37	8.00	0.210
Bi_2Te_3	0.5735	0.3727	0.50	0.48	0.015

* The concentration of In corresponding to the maximum of c parameter

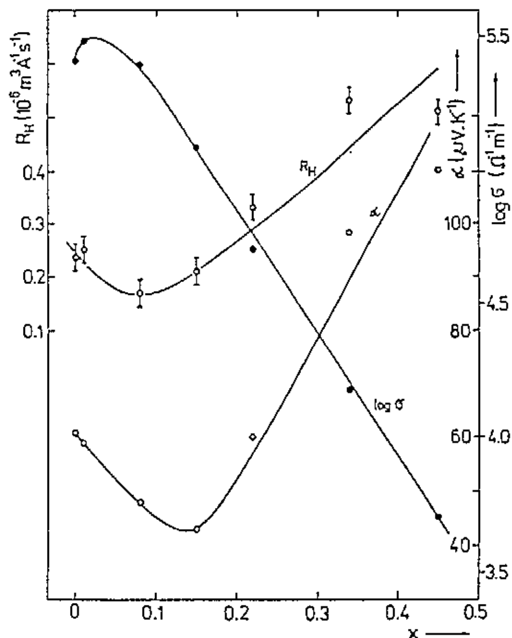

Fig. 9 The dependence of changes in the values of Hall constant R_H, Seebeck coefficient $S_{\perp c}$ and electrical conductivity $\sigma_{\perp c}$ on the content of In atoms in the samples $Bi_{2-x}In_xSe_3$

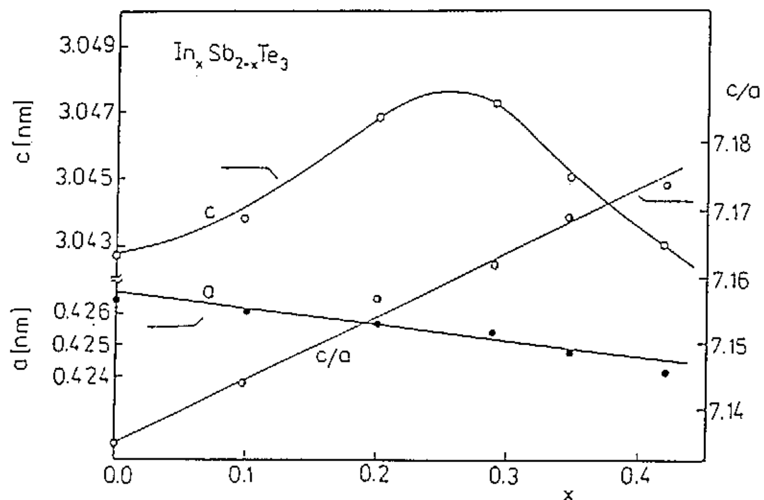

Fig. 10 The dependence of crystal lattice parameters *a* and *c* in the indium content of $Sb_{2-x}In_xTe_3$ crystals

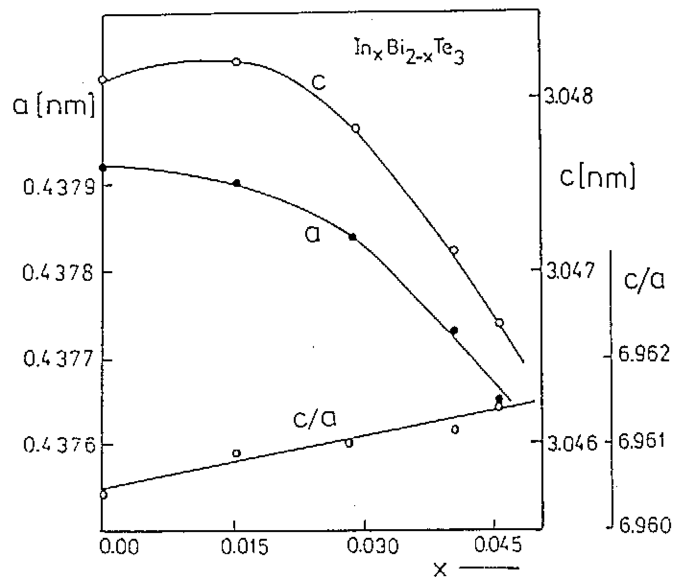

Fig. 11 The dependence of crystal lattice parameters a and c in the indium content of $Bi_{2-x}In_xTe_3$ crystals

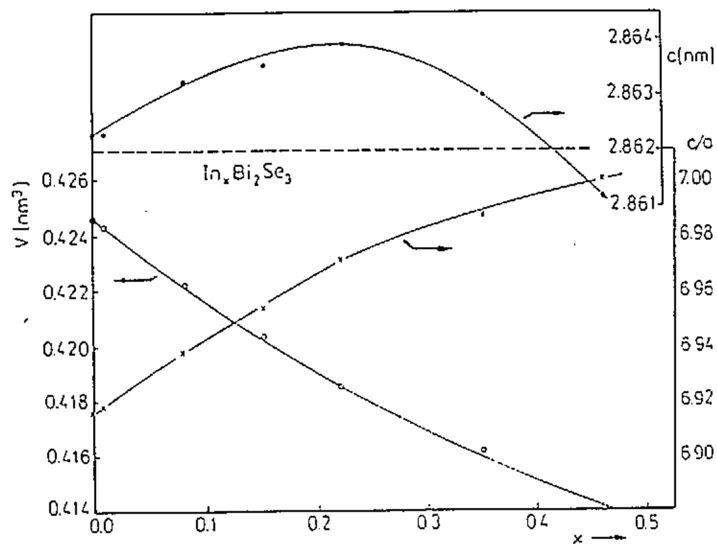

Fig. 12 The dependence of crystal lattice parameters a and c in the indium content of $Bi_{2-x}In_xSe_3$ crystals

As mentioned above the solubility of gallium chalcogenides in Bi_2Te_3 was markedly lower in comparison with indium chalcogenides. In spite of very low solubility of Ga in Bi_2Te_3 (Ref.[25]), remarkable changes in the optical and electrical properties were observed unlike the Bi_2Te_3(In) system. Table IX presents values of the transport coefficients of Bi_2Te_3(Ga) crystals at 300 K.

Table IX Values of the transport coefficients of Bi_2Te_3(Ga) crystals at 300 K and $P/m_{\perp}^*$ from reflectivity measurements

Sample No.	Conductivity type	Ga content mol %	$R_H(B \parallel c)$ 10^6 m^3 A^{-1} s^{-1}	$\sigma_{\perp c}$ 10^4 Ω^{-1} m^{-1}	$S(\Delta T \perp c)$ μV K^{-1}	$P/m_{\perp}^*$ 10^{25} m^{-3}
1	p	0.00	0.420	5.888	220	6.4
2	p	0.31	1.040	3.055	235	-
3	p	0.34	0.835	1.737	140	3.1
4	n	0.41	-0.660	1.915	-135	4.2
5	n	0.46	-0.435	5.527	-235	7.1
6	n	0.70	-0.280	7.852	-205	-

From the table it is evident that introduction of Ga atoms into the structure of Bi_2Te_3 results for low Ga concentrations in an increase of the Hall constant (see Fig. 13). After reaching a certain gallium concentration, the sign of R_H changes and a decrease in the R_H value is observed for further increasing Ga content. Introduction of gallium atoms in the crystal thus leads first to a suppression of the concentration of current carriers (holes); at a certain limiting concentration of gallium the conductivity changes from p-type to n-type and further increasing of Ga content leads in the n-type samples to an increase of the free electron concentration. The results of the measurements of the Hall constant thus imply a conclusion that the gallium impurity in the Bi_2Te_3 crystal lattice acts as a donor. The same changes in free carrier concentration can be calculated from reflectivity measurements (see Table IX).

The gallium atoms in Bi_2Te_3 crystals can play the role of donors on incorporation into the crystal lattice if they:

(a) substitute Bi atoms, with tellurium entering Te-sublattice sites - i.e. on formation of $Bi_{2-x}Ga_xTe_3$ crystals, or
(b) enter into interstitial sites where they ionize.

In the first case (a) the suppression of the concentration of holes can be explained in agreement with the ideas on incorporation of In atoms into the

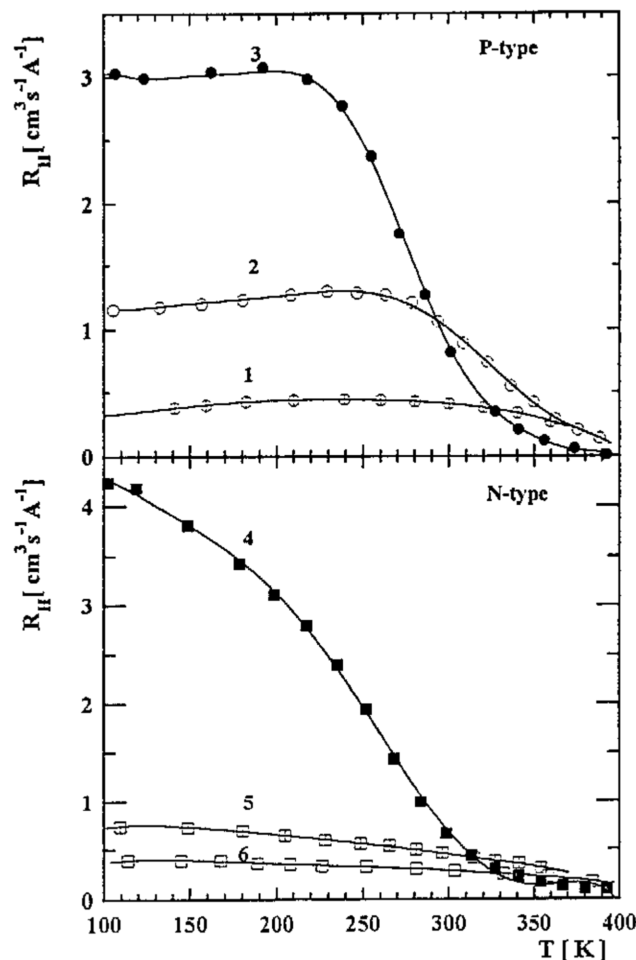

Fig.13 Temperature dependence of the Hall constant $R_H(B \parallel c)$ of Bi_2Te_3(Ga) crystals (samples are numbered in accordance with Table IX)

Bi_2Te_3 lattice leading to the formation of $Bi_{2-x}In_xTe_3$ crystals[17]. As it was mentioned above, this idea supposes a transport of two 4s electrons of Ga into p-states - i.e. a change of Ga valence electron configuration from $4s^24p^1$ to $4s^04p^3$. The uncharged substitutional defect Ga_{Bi}^x arising in this way does not lead by itself to any change in the concentration of holes, but the lower electronegativity of Ga atoms with respect to Bi (the electronegativity of Bi equals 2.02, that of Ga only 1.81) contributes to higher polarity of the bonds between the defect and the neighbouring Te atoms, i.e. the Ga_{Bi}^x-Te bonds. The higher bond polarity then results in a suppression of the formation of AS defects Bi_{Te}' whose existence is due to unpolarized bonds in the Bi_2Te_3 lattice. Qualitatively, this idea can be expressed by the following equation

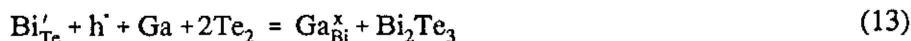

$$Bi'_{Te} + h^{\bullet} + Ga + 2Te_2 = Ga^{x}_{Bi} + Bi_2Te_3 \quad (13)$$

Equation (13) is based on the assumption that together with the Ga impurity there is also tellurium being incorporated into the lattice. This is in agreement with the experiment which was always carried out in such a way that the crystal grown corresponded to the stoichiometry expressed by the formula $Bi_{2-x}Ga_xTe_3$.

As concerns the case (b), the incorporation the Ga atoms as interstitial impurities in the lattice seems to be probable in view of the small atomic radius of Ga compared to Bi. The formation of interstitial impurities can be expressed schematically by the equation

$$Ga = Ga^{\bullet}_{i} + e' \quad (14)$$

The higher probability of the case (b) can be illustrated by Fig. 14. In this figure there are presented dependences of the free carrier concentration (obtained from the R_H-values using the formula $R_H = r\gamma/(eP)$, where $\gamma = 0.514$ according to Ref.[19] and r was taken equal to unity) on the Ga and In content, respectively. From this figure is evident that incorporation of a certain amount of Ga-atoms produces almost the same amount of electrons, which recombine in the p-type with holes and in the n-type they increase the free electron concentration.

It can be concluded that smaller Ga atoms with high probability occupy the interstitial sites unlike the In atoms that occupy the lattice sites. This fact is reflected also in the solubility of both gallium tellurides and indium tellurides in the materials studied. More detailed information on this system is covered in Refs[26,27].

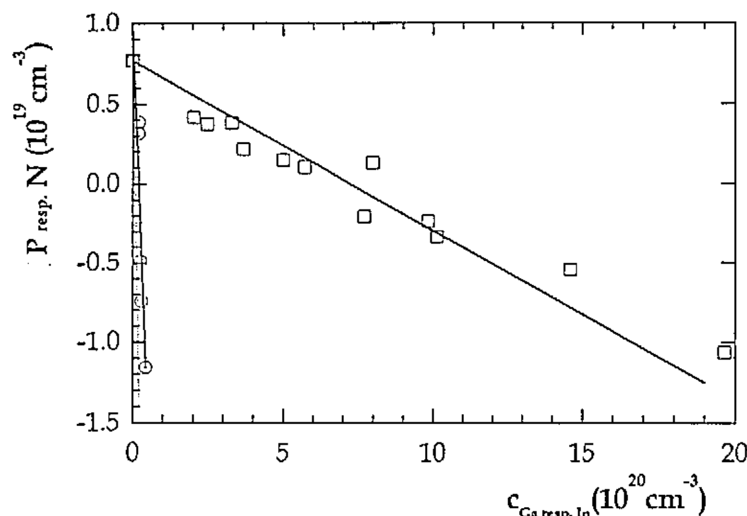

Fig. 14 Dependences of free carrier concentration on the Ga content in $Bi_{2-x}Ga_xTe_3$ single crystals (circles) and in $Bi_{2-x}In_xTe_3$ single crystals (squares). The dotted line represents an intersticial model according to Eq. 14

The Influence of IV. B Group Dopants (Ge, Sn, Pb) on the Properties of the Basic Materials

Bi_2Te_3 Crystals Doped with Germanium

Several different models describing the building-in of Ge-atoms into the Bi_2Te_3 crystal lattice, or the defects in Ge-doped Bi_2Te_3 crystals, have been presented up to now. According to the model presented in Ref.[28], the Ge impurity atoms form substitutional defects in the crystal lattice both in the cation and anion sublattice. On the other hand, in Ref.[29] a conclusion was arrived at that Bi_2Te_3(Ge) crystals with higher Ge doping level (above 0.3 at.%) contain two phases (of p- and n-type electrical conductivity); the crystals obtained are composed of the alternating layers. According to Ref.[30], the Ge impurity in the range of low concentration forms negatively charged substitutional Ge'_{Bi} defects in the Bi_2Te_3 crystal lattice, in the concentration range in excess of 3.5 at.% Ge the impurity atoms enter the van der Waals gap where they form a new atomic plane periodically repeated in the direction of the trigonal *c*-axis of the crystal. The latest views on the nature of incorporation of Ge atoms into the Bi_2Te_3 crystal lattice are presented in Refs.[31,32]. The model, which results from direct HRTEM observations, is based on the structure of Bi_2Te_3, formed by five-layer lamellae Te-Bi-Te-Bi-Te bonded one to another by van der Waals forces. The incorporation of Ge results in the formation of seven-layer lamellae of the composition Te-Bi-Te-Ge-Te-Bi-Te, which formally correspond to the compound $GeBi_2Te_4$.

The results of free carrier concentration calculated from reflectivity measurements of Bi_2Te_3(GeTe) single crystals (by means of Eqs (3) - (7) and using the value $m_{\perp}^{*} = 0.08m_0$ (Ref.[33])) together with electrical conductivity values at 300 K are presented in Table X. It is evident from this table that the presence of Ge impurity atoms in the Bi_2Te_3 lattice causes an increase in the concentration of free carriers. In view of the fact that the starting undoped Bi_2Te_3 exhibits p-type electrical conductivity, one can accept an important conclusion that Ge atoms in Bi_2Te_3 lattice play a role of acceptors. This fact is also supported by the results of the electric conductivity measurements; its value increase with the increasing Ge content in the samples.

Atoms of any impurity, hence also Ge atoms, can be built into Bi_2Te_3 crystal lattice in one of the following ways:

a) by substitution of Bi atoms, i.e. incorporation into the cation sublattice
b) by substitution of Te atoms, i.e. incorporation into the anion sublattice
c) by occupation of sites in the van der Waals gap
d) by occupation of interstitial sites in the crystal lattice, i.e. formation of interstitial ions.

Case (d) need not be taken into account as the interstitial atoms would be

Table X Parameters characterizing single-crystalline $Bi_2Te_3(GeTe)$ samples

c_{Ge} 10^{21} cm^{-3}	$\sigma_{\perp c}$ 10^{13} Ω^{-1} m^{-1}	ω_p 10^{13} s^{-1}	P 10^{18} cm^{-3}	$\Delta P = P - P_0$ 10^{18} cm^{-3}	$c_{Ge}/\Delta P$
0.00	66.07	6.42	5.12 = P_0	0.0	-
1.00	251.19	9.40	16.6	11.5	87
1.20	301.99	9.10	15.5	10.4	115
1.90	354.80	11.60	24.8	19.7	96
2.19	389.04	11.10	22.6	17.5	125
2.29	407.38	11.60	27.4	22.3	103

ionized and behave thus like donors, which is at variance with experiment. Also different character of both elements, in our opinion, prevents Ge atoms from the substitution for atoms in Te sublattice.

The acceptor-like behaviour of the Ge atoms is most probably due to their incorporation into the Bi sublattice (case (a)), where they give rise to negatively charged substitutional defects Ge'_{Bi} whose charge is compensated by holes, which results in an increase in the concentration of free carriers. The process of formation of the defects of this type can be represented by the equation

$$(2\,V_{Bi} + 3\,V_{Te})^x + 2\,Ge + 3/2\,Te_2 = 2\,Ge'_{Bi} + 2\,h^{\bullet} + 3\,Te_{Te} \tag{15}$$

The equation assumes that Te enters the crystal lattice together with Ge. The required superstoichiometric Te was added to the melt, from which the crystals were pulled, as GeTe and further as Te, which segregates during the growth of p-Bi_2Te_3 crystals exhibiting Bi superstoichiometry (see e.g. Ref.[3]).

In ordert to judge whether all incorporated Ge atoms form above-mentioned subtitutional defects or a part of the impurities cannot be built into the crystal lattice in some other way, the change of free carrier concentration with the Ge content in the samples was calculated. From ΔP values ($\Delta P = P_0 - P$, where P_0 is the concentration of free carriers in "pure" Bi_2Te_3 and P is that in the samples) and from Ge content, c_{Ge} values, a $c_{Ge}/\Delta P$ ratio was determined (see Table X). As it is evident from the last column in the table, the increase by one hole in the free carrier concentration is connected with the incorporation of about 100 Ge atoms i.e. approximately 1 atom out of 100 enters the Bi_2Te_3 crystal lattice in the form of a Ge'_{Bi} defect in the sense of Eq. (15). This fact can lead to a conclusion that only a small portion of the total number of Ge atoms forms negatively charged Ge'_{Bi} defects in the crystal lattice, the remaining Ge probably entering the van der Waals gap. Accepting the model proposed in Ref.[31] it seems plausible to adopt the idea that Ge atoms form seven-layer lamellae Te-Bi-Te-Ge-Te-Bi-Te.

Also the following effect observed on analyzing the Ge content by means of EDX analyzer can support, in our opinion, the proposed conclusion on the nature of incorporation of Ge atoms into Bi_2Te_3 crystal lattice. This effect is obvious from Fig. 15, where two EDX spectra of the sample studied (sample with Ge content of 1.9×10^{21} cm^{-3} in Table X) are compared. While in the spectrum taken from the natural cleavage face of the single crystalline sample there are no bands of X-ray radiation characteristic of Ge, after grinding of single crystal into a fine powder, besides the bands corresponding to Bi and Te also lines of Ge appear in the spectra. It seems plausible to accept the following qualitative explanation of the observed phenomenon. If the overwhelming majority of Ge atoms forms seven-layer lamellae, the crystals will be well cleavable along the van der Waals gap, i.e., in those places where there are no seven-layer lamellae. Taking into account the fact that the characteristic X-ray radiation is strongly absorbed (or scattered) by the Bi_2Te_3 lattice, the analysis of the single crystalline sample yields data on the Ge content in the cleavage plane, or in the region close to its surface. Then, one cannot exclude the possibility that in this part of the sample the content of Ge - which is here incorporated in the form of Ge'_{Bi} defects - lies below the detection limit of the EDX analysis and that is why no lines corresponding to the characteristic radiation of Ge are found in such spectrum. After grinding, however, the resulting material yields information about the composition of the whole bulk sample, i.e., the characteristic radiation lines of Ge are well visible in the spectrum.

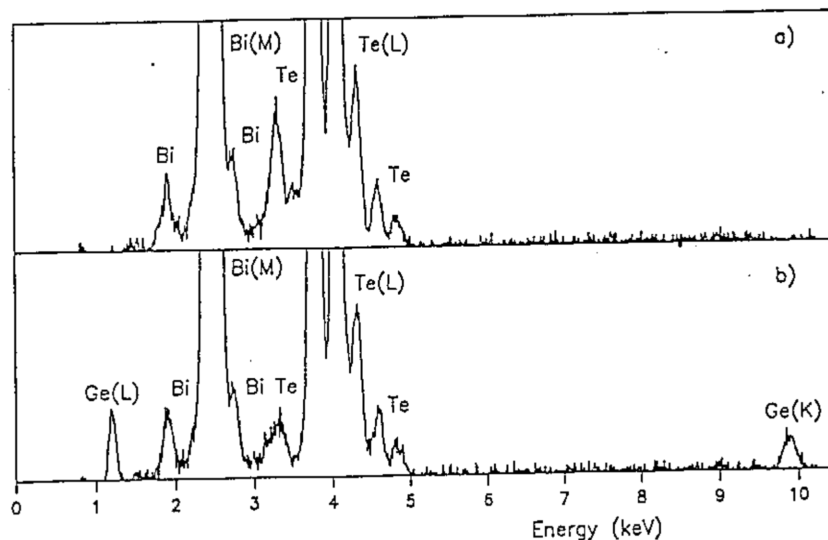

Fig.15 EDX spectra of a $Bi_2Te_3(GeTe)$ sample with a Ge content of 1.9×10^{21} cm^{-3}: a - spectrum taken from the natural cleavage face of the single-crystalline sample, b - spectrum taken from a powder sample obtained by grinding the single crystal

The following conclusion can be drawn from the above-mentioned facts: Ge atoms form most probably substitutional defects Ge'_{Bi} which account for the acceptor nature of this impurity, as well as new atomic layers formed by Ge atoms entering the van der Waals gap, which lead probably to the formation of seven-layer lamellae Te-Bi-Te-Ge-Te-Bi-Te.

Bi_2Te_3 Crystals Doped with Tin

As it follows from Ref.[34], unlike in the above-mentioned system (Bi_2Te_3 with Ge), solubility of tin in Bi_2Te_3 is markedly lower. Nevertheless, the changes of some transport and optical properties caused by the incorporation of tin atoms into Bi_2Te_3 crystal lattice are very similar to those in the case of Ge impurity. Also here the authors suppose that the observed increase of hole concentration resulting from incorporation of Sn atoms can be connected with formation of negatively charged substitutional defects Sn'_{Bi}. The entering of Sn atoms into the Bi_2Te_3 lattice can be described qualitetively by Eq. (15), where Ge atoms are replaced by Sn atoms. Comparing Sn content in Bi_2Te_3 crystals with the changes of free carrier concentrations (they were calculated from the Hall measurements and also from the measurements of reflectivity[34]), one can conclude that not every built-in Sn atom contributes to the change of free carriers concentration, i.e. that a part of built-in Sn atoms give rise to electrically inactive point defects. As in the case of Ge in Bi_2Te_3 the authors suppose that one part of built-in Sn atoms form substitutional defects Sn'_{Bi} and the other part form seven-layer lamellae Te-Bi-Te-Sn-Te-Bi-Te.

In our work[35] we have studied a structure of Sn-doped Bi_2Te_3 crystals by means of Augere depth profile analysis and high resolution transmission electron microscopy (HRTEM - Philips CM 30 FEG, 300 kV, 0.23 nm) with EDX analyzer (EDAX 9900). The single crystals of Bi_2Te_3 with Sn content of 0.3, 0.5, 1 and 2 at. % were prepared. The Augere depth profile analysis from cleavage planes down to the depth of about 3000 Å was carried out. The depth resolution of the Augere profiling was 2-3 nm. From these measurements it follows that the Sn atoms do not form any separate phase or any layers of pure Sn within the whole thickness of the samples, i.e., they are homogeneously dissolved in Bi_2Te_3. From HRTEM measurements of the samples it is evident that the Sn dopant gives rise to two different structural modifications of the basic material, depending on the concentration of the Sn atoms. Up to a concentration of approximately 0.4 at.% Sn, the Sn substitutes Bi atoms in the Bi_2Te_3 lattice, and the structure is identical with that of Bi_2Te_3. When more Sn was added, regions of higher Sn concentration formed, where a completely new lattice structure could be found. Beside five-layer packets normally presented in the structure of Bi_2Te_3 there are some seven-layer lamellae (probably of Te-Sn-Te-Bi-Te-Sn-Te or Te-Bi-Te-Sn-Te-Bi-Te type) observed on the HRTEM pictures. Randomly distributed seven-layer structures among five-layer structures

come into existence at first. When the Sn content increases, the number of seven-layer structures increases too, and after reaching a certain concentration a regular arrangement of alternating five- and seven-layer structures can be found, i.e., the superstructure comes into existence. These seven-layer structures could be identified from satellite peaks found in diffraction patterns of the sample, directly from image, and most clearly from the diffractograms of the images obtained from TEM-micrographs by means of 2-D Fourier Transform. Figures 16 and 17 present the TEM-micrograph of the sample with high Sn concentration and diffractogram of the image.

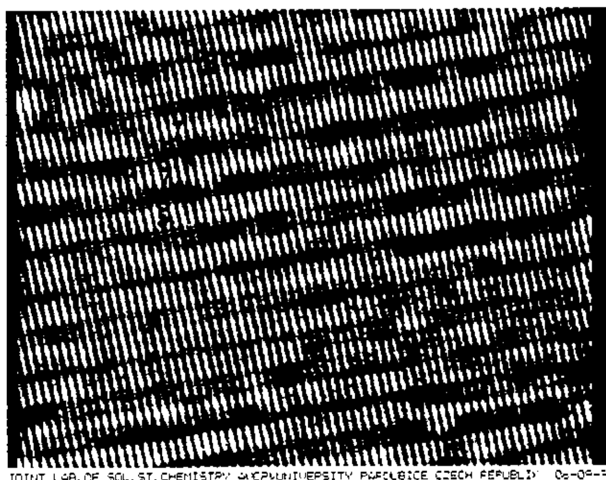

Fig.16 HRTEM picture of Bi_2Te_3 doped with 2 at.% of Sn. An arrangement of alternating five- and seven-layer lamellae structures is indicated.

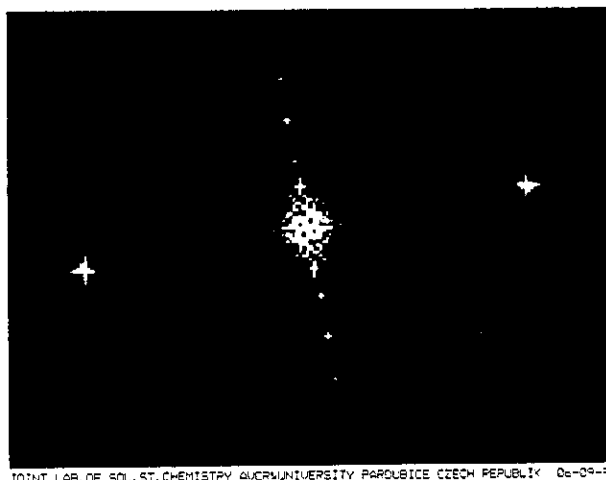

Fig. 17 The diffractogram obtained from Fig. 16 by means of 2-D Fourier Transform

The Influence of V. B Group Dopants (Bi) on the Properties of the Basic Materials

$Bi_{2+x}Te_3$ *and* $Bi_{2+x}Se_3$ *Crystals*

Clarification of the nature of point defect and, in particular, of their charge in $Bi_{2+x}Te_3$ and $Bi_{2+x}Se_3$, i.e., in crystals exhibiting a considerable departure from stoichiometry and their relation with some physical properties of these crystals are presented in paper[36].

The bismuth telluride crystals prepared by the Bridgman technique from the stoichiometric melt show a superstoichiometric Bi content, a p-type electrical conductivity and a hole concentration of approx. $6-7\times10^{18}$ cm^{-3}; the bismuth selenide crystals prepared from the melt corresponding to the Bi_2Se_3 stoichiometry also exhibit Bi stoichiometry. Bi_2Se_3 crystals are always of the n-type with electron concentration of about $1-2\times10^{19}$ cm^{-3}.

According to the authors[19,37] the connections between bismuth superstoichiometry and free carrier concentration in Bi_2Te_3 crystals are explained by formation of AS defects of Bi'_{Te}-type, formed during the crystal growth. These AS defects are compensated by holes. The n-type conductivity of Bi_2Se_3 crystals is accounted for by the existence of positively charged selenium vacancies $V^{\bullet}_{Se}$ (Ref.[38]), whose charge is compensated by electrons. However, this simple idea on the influence of superstoichiometric bismuth in Bi_2Se_3 is not sufficient to explain the changes of electron concentration in Bi_2Se_3 crystals with various amounts of Bi in the lattice. Bi_2Se_3 crystals prepared from the melt with superstoichiometric bismuth content always show a decrease of free electron concentration, when the x value in $Bi_{2+x}Se_3$-melt increases (see Table XI). This phenomenon is - in our opinion - relevant and its observation suggests the existence of AS defects in Bi_2Se_3 crystals, which has been formulated in work[11]. Therefore, the phenomenon described can be considered as another circumstantial evidence of the existence of AS defects Bi'_{Se}-type in Bi_2Se_3 crystals.

The influence of the superstoichiometric bismuth content in Bi_2Se_3 and Bi_2Te_3 crystals would then be the same. According to Brebrick[19] and also Che-Yu Li[37], superstoichiometric Bi atoms in Bi_2Te_3 crystals enter into the tellurium sublattice and form AS defects Bi'_{Te}. It is in agreement with the experiment (see Table XI) in which Bi_2Te_3 crystals prepared from Bi-rich melt exhibit an increase in hole concentration.

Thus, the electron conductivity of $Bi_2Se_3(Bi)$ and hole conductivity of $Bi_2Te_3(Bi)$ can be explained by taking into account two kinds of defects, i.e., AS defects and vacancies in the anion sublattice, which determine the free carrier concentration. The free carrier concentration is approximately given by the equations

Table XI Optical parameters of $Bi_{2+x}Te_3$ and $Bi_{2+x}Se_3$ single crystals calculated from reflectance spectra

Melt composition	λ_{min} μm	$\omega_p(E \perp c)$ 10^{13} s^{-1}	$N/m_{\perp}^*$ 10^{25} m^{-3}	N^x 10^{25} m^{-3}
$Bi_{2+x}Te_3$ (x = 0.00)	28.1	5.84	8.958	0.716
$Bi_{2+x}Te_3$ (x = 0.25)	14.7	10.50	23.180	1.854
$Bi_{2+x}Se_3$ (x = 0.00)	12.9	13.75	17.571	2.178
$Bi_{2+x}Se_3$ (x = 0.20)	14.9	11.88	14.657	1.817
$Bi_{2+x}Se_3$ (x = 0.25)	16.5	10.63	12.550	1.556

$$\begin{aligned} &\text{in p-}Bi_2Te_3 : \quad [h^{\cdot}] = [Bi'_{Te}] - [V^{\cdot}_{Te}] \\ &\text{in n-}Bi_2Se_3 : \quad [e'] = [V^{\cdot}_{Se}] - [Bi'_{Se}] \end{aligned} \quad (16)$$

The formation of AS defects of the Bi'_{Se}-type in Bi_2Se_3 does not contradict the bonding picture; in agreement with the results reported in paper[24] the polarity of the bonds $Bi-Se^2$ is lower than that of the $Bi-Te^2$ bonds. The finding of a lower bond polarity of the $Bi-Se^2$ bonds, compared to that of the $Bi-Te^2$ bonds, is in agreement with the experimentally determined values of the energy of formation of AS defects, $E_0(Bi'_{Se})$ and $E_0(Bi'_{Te})$, reported in Ref.[39].

Both the experimental results and the calculated bonding parameters support the view that superstoichiometric Bi atoms in the Bi_2Se_3 lattice favour the formation of AS defects of the Bi'_{Se} type. It is, however, well known that one of the conditions for the formation of a substitutional defect is the suitable size of the atomic radius; the covalent radius of the selenium atom, r_{Se}, is smaller than the covalent radius of the bismuth atom, r_{Bi} (r_{Se} = 1.17 Å, r_{Bi} = 1.51 Å). Nevertheless, in view of the significant contribution of covalent bonding, it is necessary to take into account the electron density corresponding to the atoms in Se^1, Se^2 and Bi sites; the electron density influences the "effective" radius of both selenium and bismuth. With the aim to estimate the variations of the radii of Se^1, Se^2 and Bi atoms, a strongly simplified idea of the proportionality between the atomic charge and the "effective" radius of a covalently bonded atom was used. On this assumption one can find from the dependence of 'effective' radius vs. atomic charge (a linear dependence between covalent and ionic radius of Bi and Se was taken into account, the charges of Bi, Se^1 and Se^2 were calculated by means of quantum-chemical calculation) following values of effective radii: $r(Se^1)_{Bi_2Se_3}$ = 1.52 Å, $r(Se^2)_{Bi_2Se_3}$ = 1.23 Å, $r(Bi)_{Bi_2Se_3}$ = 1.31 Å. On the basis of this semiquantitative argument we

conclude that the condition of similarity of atomic radii between Bi and Se[1] atoms for the formation of AS defects is also fulfilled.

Some new ideas, based on the results of investigations of layered structures by means of UHREM[31,32] indicate, however, that the superstoichiometric Bi content could be realized in a way differing from the idea of simple point defects like Bi'_{Te} and Bi'_{Se}. Let us assume, according to Refs[31,32], that the excess Bi atoms in Bi_2Te_3 or Bi_2Se_3 lattice participate in the formation of an extra seven-atom stack, the so-called seven-layer lamella, with the sequence Te-Bi-Te-Bi-Te-Bi-Te, which is intercalated between the standard five-atom stacks Te-Bi-Te-Bi-Te of the tetradymite structure.

However, the papers[31,32] do not specify which relations exist between the superstoichiometric bismuth content, belonging to seven-layer lamella, and the charge. The magnitude of the charge can be deduced on the basis of a bonding concept formulated by Krebs: only $5p^3$-electrons of Bi and $4p^4$-electrons of Te participate in the chemical bond between Bi and Te atoms. Assuming similarity of structure and bond between the seven-layer lamella and tetradymite structures, it can be assumed that each seven-layer lamella $(Bi_3Te_4)_n$ causes changes in electronic system of the lattice. The addition of Bi-Te to the normal five-layer unit might be considered as a Te deficit with respect to the stoichiometric composition, i.e., a deficit in bonding electrons. Excitation of valence electrons to fill these bound holes would generate free holes in the valence band.

The "polarization" model allows us to perform also the quantitative calculations. In Ref.[22] the calculations of the concentration of different kinds of AS defects were performed on the $Bi_2Te_3 - Sb_2Te_3$ system on the basis of "polarization" model and quantum chemical calculations. The system forms mixed crystals in all concentration regions. In Fig. 18 one can see the calculated concentration of both Sb'_{Te} and Bi'_{Te} AS defects in mixed crystals $Bi_2Te_3 - Sb_2Te_3$ as a function of Bi_2Te_3 concentration. In the region of about 25% Bi_2Te_3 the maximum of the Bi'_{Te} defect concentration occurs. One can assume that in this region the $Bi_2Te_3 - Sb_2Te_3$ system shows in this region some pronounced changes in its physical properties. Certain effects appearing at the above concentration of Bi_2Te_3 have been reported in paper[11] where the author mentions, above all, marked variations in the effective mass curve. Also in Ref.[40] the minimum of heat conductivity is mentioned in this concentration region. We can see that the calculations could be very important for the construction of the optimum Peltier element.

The Influence of VI. B Group Dopants (Se) on the Properties of the Basic Materials

$Sb_2Te_{3-x}Se_x$ Single Crystals

In order to estimate qualitatively the nature of point defects in the $Sb_{2-x}Te_{3-x}Se_x$ crystals, the changes in the free carrier concentration have been determined from the values of the Hall constant and reflectivity measurements (see Table XII). The results of independent measurements of reflectivity, the Hall constant and electric conductivity lead us to conclude that the incorporation of Se atoms into the crystal lattice of Sb_2Te_3 is responsible for a decrease in the free carrier concentration. The suppression of the free carrier concentration can be accounted for on the basis of simple ideas about the point defects in crystalline solids. The selenium atoms in $Sb_2Te_{3-x}Se_x$ crystals substitute tellurium atoms in lattice sites and form uncharged Se_{Te}^{x} defects, because they have the same number of valence electrons as Te atoms. As mentioned above, the Sb_2Te_3 crystal exhibits relatively high concentration of AS defects Sb'_{Te}. Their formation can be qualitatively described by the equation

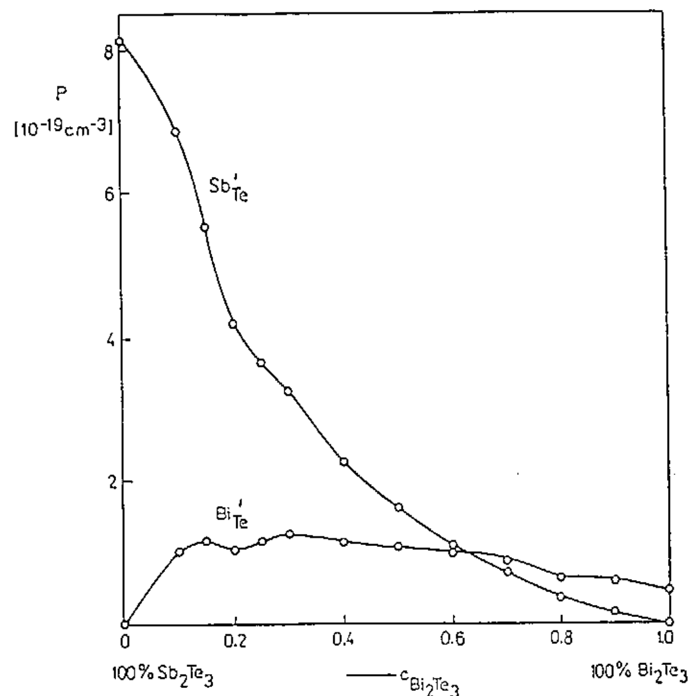

Fig.18 Calculated dependence of antisite defect concentration in $(Bi_2Te_3)_{1-x}(Sb_2Te_3)_x$ solid solutions

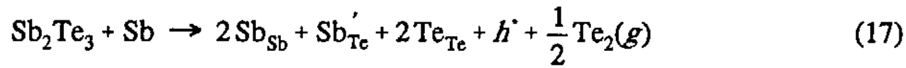

$$Sb_2Te_3 + Sb \rightarrow 2Sb_{Sb} + Sb'_{Te} + 2Te_{Te} + h^{\bullet} + \frac{1}{2}Te_2(g) \qquad (17)$$

A shift in this equilibrium in favour of the formation of AS defects, or of their suppression, can be provoked by an increase, or decrease, in the bond polarity. The Se atoms enter the Sb_2Te_3 crystal lattice by occupying the sites in the tellurium sublattice, thus forming substitutional Se^{x}_{Te} defects. Due to a higher electronegativity of selenium against tellurium, these defects carry a partial negative charge $Se^{(-\delta)}_{Te}$. For this reason, the bonds between $Se^{(-\delta)}_{Te}$ and Sb atoms are more polar than the original Te-Sb bonds. Enhanced polarity of the bonds then results in a suppression of the formation of AS defects Sb'_{Te} and, hence, in a decrease of hole concentration by shifting the equilibrium (17) to the left.

Table XII Plasma resonance frequency, electrical conductivity and Hall coefficient of $Sb_2Te_{3-x}Se_x$ crystals at 294 K

x in $Sb_2Te_{3-x}Se_x$	$\omega_p(E \perp c)$ 10^{14} s^{-1}	$\sigma_{\perp c}$ 10^5 Ω^{-1} m-1	$R_H(B \parallel c)$ $cm^3 A^{-1} s^{-1}$	$P(\sim 1/R_H e)$ 10^{19} cm^{-3}
0.00	1.88	5.10	0.057	10.95
0.09	1.81	3.30	0.088	7.09
0.38	1.62	2.03	0.144	4.33
0.47	1.55	1.79	0.145	4.30
0.63	1.45	1.61	0.167	3.74
0.99	1.16	2.49	0.248	2.52
1.25	0.99	2.15	0.335	1.86

Figure 19 shows how important the knowledge of these facts can also be for the applications of these materials. To study a strong doping of Sb_2Te_3 with Se, the exposition of Sb_2Te_3 single crystals in Se vapours has been carried out, see Ref.[41]. Contrary to all expectations, p-n junction was observed in this structure. Similar problems were discussed also for $Bi_2Te_3 - Bi_2Se_3$ system in Ref.[42]. Figure 19 shows the current-voltage characteristic of the prepared structure. Evidently, the characteristic is typical of p-n junction. This is very interesting, because both Sb_2Te_3 and Sb_3Se_3 are p-type semiconductors and, as far as we know, there have previously been no published results concerning n-type Sb_2Te_3 in the literature. It could be proposed that the suppression of AS defects concentration at the surface by a strong doping of Se atoms is of such a magnitude that the change of conductivity type is possible.

The studied materials are widely used for the construction of both p- and n-type branches of Peltier elements. One of preparation methods is cold pressing of powdered materials and their subsequent annealing. This method is considerably cheaper and more flexible in comparison with other methods used for preparation of Peltier elements, although it yields materials of slightly lower thermoelectric quality. That is why it is important to study these materials from the point of view of their crystal defects. Some technological steps of this method influenced strongly the transport properties of these materials, and the changes observed could be explained on the basis of the above-mentioned polarization theory.

The bulks of the $Bi_{1.8}Sb_{0.2-x}In_xTe_{2.85}Se_{0.15}$, where $x = 0 - 0.02$, were prepared from elemental Bi, In, Sb, Se and Te of 5N purity. Samples were synthesized in quartz ampoules by heating at 730 °C for 48 h. The samples were pulverized and sieved to the grain size of < 32 μm, 32 - 50 μm, 50 - 80 μm, 80 - 130 μm, 130 - 300 μm and 300 - 515 μm. After grinding and cold

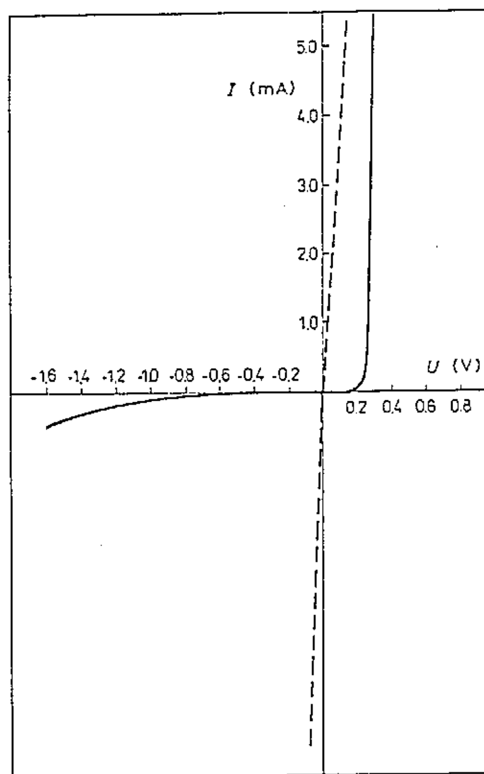

Fig. 19 Current-voltage characteristic of the $Sb_2Te_2 - Sb_2Te_{3-x}Se_x$ (dashed line - current-voltage characteristic of Ag-paste contact)

pressing the temperature dependences of electrical conductivity, the Seebeck coefficient, and the thermoelectric figure of merit in the temperature range of about 100 - 400 K were measured on the tablets.

Besides the influence of indium on the free carrier concentration which has been described above, the influence of particle size is evident from Figs 20, 21. In this case, the grinding of the samples causes an increase in the electron

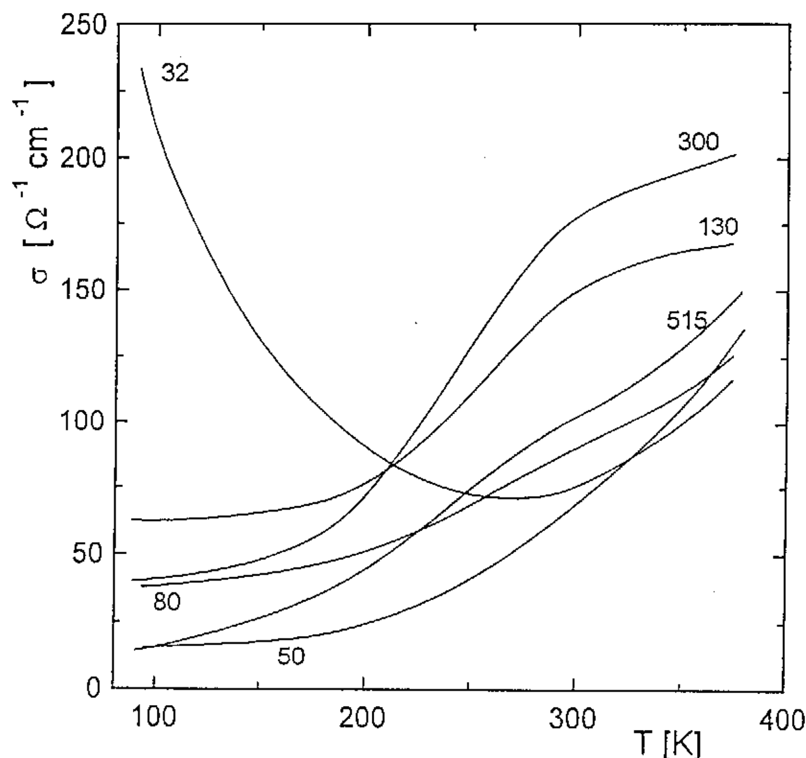

Fig. 20 Temperature dependence of the electrical conductivity of the $Bi_{1.8}Sb_{0.2}Te_{2.85}Se_{0.15}$ (size of particles: 32 - 515 μm)

concentration and a decrease in the hole concentration. As shown in Fig. 21, the grinding of samples under 50 μm changes the type of conductivity. In bulks doped with indium and thus with suppressed hole concentration nothing but grinding leads to the conductivity type inversion. Figure 22 shows values of the Seebeck coefficient for the samples with varying composition at room temperature. It is obvious that all materials before the grinding are P-types. After the grinding and pressing, the values of their Seebeck coefficient decrease (in some samples an inversion of the conductivity type occurs) and after sintering all samples are of N-type. Consequently, the sintering causes the further increase of electron concentration. What is the explanation of this phenomenon? The authors[43] propose the following explanation. By a mechanical

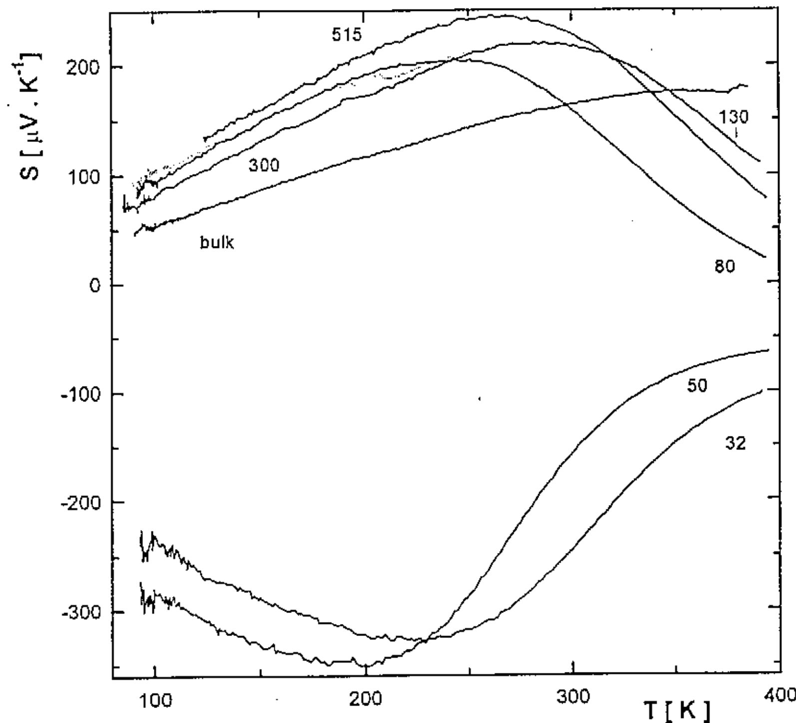

Fig. 21 Temperature dependence of the Seebeck coefficient of the $Bi_{1.8}Sb_{0.2}Te_{2.85}Se_{0.15}$ (size of particles: 32 - 515 μm)

treatment crossing dislocations, which give vacancies $V'_{Bi(Sb)}$ and $V^{\bullet}_{Te}$, are produced. The ratio of cation vacancies/anion vacancies is about 2/3. Considering one charged vacancy, the positively charged $V^{\bullet}_{Te}$ prevail. Smaller mobility of these vacancies, in comparison with the mobility of V'_{Bi} vacancies, causes their movement toward grain surface more slowly during the sintering. Thanks to this fact a surplus of positively charged defects compensated with electrons comes into existence. In our opinion, this explanation seems to be unacceptable for the following reason. If it were a kinetic phenomenon, after a long-term annealing a repeated decrease in the electron concentration would have to be observed as the $V^{\bullet}_{Te}$ vacancies move toward grain surface. However this is not observed. In connection with AS defects which occur in crystals mentioned in considerable concentration, a following explanation can be proposed. By grinding of the crystals a rise of vacancy concentration in stoichiometric ratio really occurs. These, however, do not diffuse to the grain boundaries but interact with AS defects according to the following equation

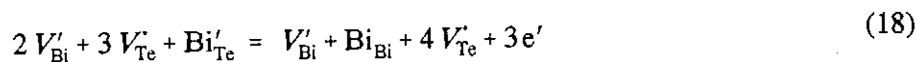

$$2\,V'_{Bi} + 3\,V^{\bullet}_{Te} + Bi'_{Te} = V'_{Bi} + Bi_{Bi} + 4\,V^{\bullet}_{Te} + 3\,e' \tag{18}$$

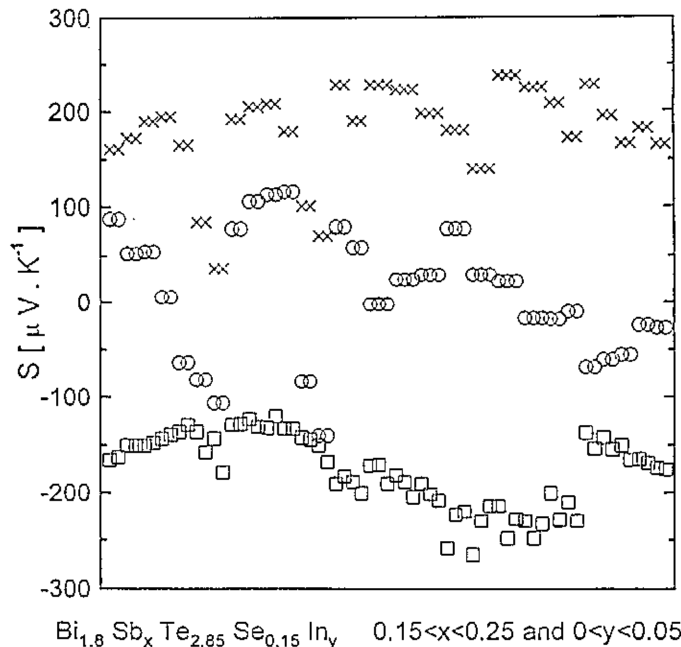

Fig. 22 The Seebeck coefficient at room temperature of several compositions of thermoelectric materials (x - synthesized, ○ - ground, □ - sintered)

In other words the Bi atom jumps from Te-sublattice to the vacancy in Bi-sublattice and Te-vacancy simultaneously comes into existence. The resulting Te-vacancies are compensated with free electrons. This process has a considerable effect and it is able to invert the conductivity type (Fig. 21) or to cause a semiconductor degeneration (Fig. 20). A considerable influence of the process on the increase in the free electron concentration is obvious also from the fact that the electrical conductivity of N-type samples increases with decreasing particle size regardless of increasing contact resistance of grains[44].

Authors[44] show that the particle size of the samples, whose free carrier concentration is located in the region of P-N transition or its nearest neighbourhood, has the greatest influence on the values of the Seebeck coefficient. In bulks with the suppressed concentration of AS-defects, i.e., suppressed hole concentration, the particle size has not such a marked influence on the thermoelectric properties (see Fig. 23).

From the technological point of view, the considered dependence of the figure of merit on the particle size is not advantageous because it also means a considerable sensibility to the preparation conditions. On the other hand, it is possible to prepare the Peltier elements with the gradient of the particle size (functionally graded materials). In this way, the figure of merit of thermoelectric materials can be optimized without any hazard of the dopant diffusion, because the starting material can be of the same composition.

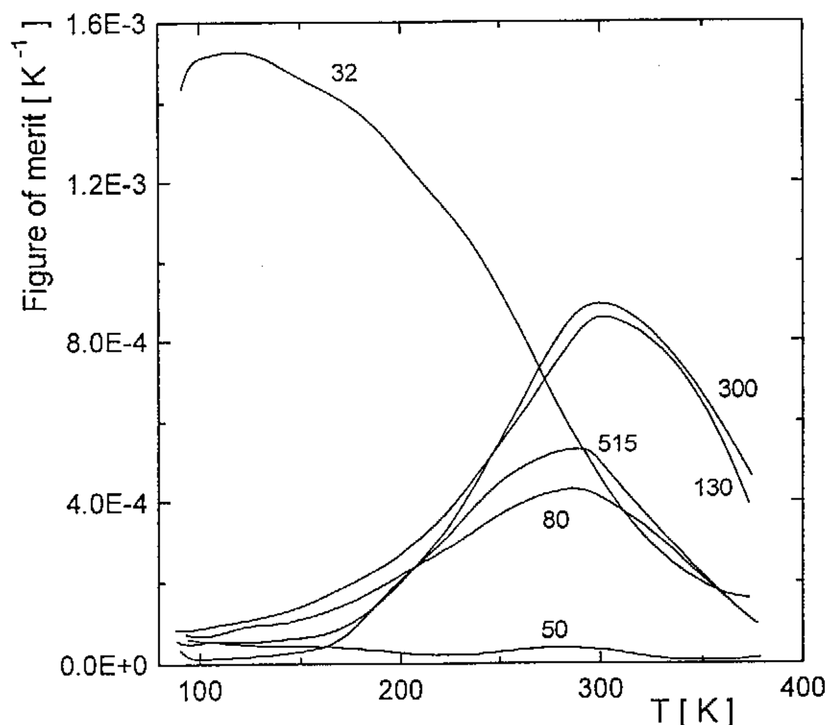

Fig. 23 Temperature dependence of the thermoelectric figure of merit of the $Bi_{1.8}Sb_{0.2}Te_{2.85}Se_{0.15}$ (size of particles: 32 - 515 μm)

Conclusion

It is evident from the results presented that the dominant type of point defects in the layered crystals with tetradymite structure A_2B_3 (and their solid solutions) is the AS defects of A'_B-type. It is obvious that the presence of these defects in crystal lattice influnces the transport properties of the materials to a considerable extent (mainly in Bi_2Te_3 and Sb_2Te_3). However, in some cases it is necessary to consider another type of defects (vacancies). The latest results indicate the existence of new type of defects - planar defects in the form of multilayered lamellae.

The measurements of transport and optical properties give a great opportunity to observe the changes in the free carrier concentration. Together with another chemical view they give the possibility to determine the nature of defects. But it seems to be necessary for the following research to select another chemical experimental method together with a initial calculations. In our opinion the study of chemical diffusion processes in this materials could by one of the suitable method.

References

1. Ioffe A.F.: *Semiconductor Thermoelements and Thermoelectric Cooling*, Infosearch, London 1957.
2. Ioffe A.F., Airapetiants S.V., Ioffe A.F., Kolomoets N.V., Stil'bans L.S.: Dokl. Akad. Nauk SSSR **106**, 981 (1956).
3. Goltsman B.N., Kubinov V.A., Smirnov I.A.: *Poluprovodnikovyje termoelektricheskije materialy na osnove Bi_2Te_3*, Izd. Nauka, Moskva 1972.
4. Rowe D.M., Bhandari C.M.: *Modern Thermoelectics*, Holt, Rinehart and Winston Ltd. 1983.
5. Šrámková J., Kotrlý S.: Talanta **35**, 841 (1988).
6. Rosenberg A.J., Strauss A.J: J. Phys. Chem. Solids **19**, 105 (1961).
7. Lošťák, L. Beneš, S. Civiš and H. Süssmann: *J. Mater. Sci.*, **25**, 277 (1990)
8. Lošťák P., Novotný R., Horák J., Klikorka J.: Phys. Status Solidi **A 89**, K55 (1985)
9. Moss T.S., Burrell G.J., Ellis E.: *Semiconductor Opto-Electronics*, p. 43, Butterworths, London 1973.
10. Stordeur M., Simon G.: Phys. Status Solidi **B 124**, 799 (1984).
11. Stordeur M.: *Thesis B*, Univ. Halle-Wittenberg 1986.
12. Pancíř J: Coll. Czech. Chem. Comm. **45**, 2452 (1980).
13. Pancíř J., Haslingerová I., Nachtigall P.: Surface Science **181**, 413 (1987).
14. Horák J., Lošťák P., Beneš L.: Phil. Mag. **B 50**, 665 (1984).
15. Horák J., Čermák K., Koudelka L.: J. Phys. Chem. Solids **47**, 805 (1986).
16. Horák J., Lošťák P., Koudelka L., Novotný R.: Solid State Commun. **55**, 1031 (1985).
17. Lošťák P., Horák J., Koudelka L.: Phys. Status Solidi **A 76**, K71 (1983).
18. Horák J., Starý Z., Lošťák P., Pancíř J.: J. Phys. Chem Solids **49**, 191 (1988)
19. Brebrick R.F.: J. Phys. Chem. Solids **30**, 719 (1969).
20. Horák J., Navrátil J., Starý Z.: J. Phys. Chem. Solids **53**, 1067 (1992).
21. Krebs H.: *Grundzüge der Anorganischen Kristallchemie*, p. 239, Stuttgart (1968)
22. Starý Z., Horák J., Stordeur M., Stölzer M.: J. Phys Chem. Solids **49**, 29 (1988).
23. van Vechten J. A.: J. Electrochem. Soc. **122**, 419 (1975).
24. Horák J., Starý Z., Lošťák P., Pancíř J.: J. Phys. Chem. Solids **51**, 1353 (1990).
25. Rustamov P.G., Seidova N.A., Shakhbazov M.G.: Zh. Neorg. Khim. **21**, 764 (1976).
26. Lošťák P., Novotný R., Navrátil J., Šrámková J.: Phys. Status Solidi **A 106**, 619 (1988).
27. Navrátil J., Lošťák P., Horák J.: Cryst. Res. Technol. **26(6)**, 675 (1991).
28. Bergman G.: Naturforchung **18a**, 1169 (1963).
29. Tamura H.: Japan J. Appl. Phys. **7**, 593 (1966).

30. Předota M, Beneš L., Horák J.: Phys. Status Solidi **A100**, 401 (1987).
31. Frangis N., Kuypers S., Manolikas C., van Landuyt J., Amelinckx S.: Solid State Commun. **69**, 817 (1989).
32. Frangis N., Kuypers S., Manolikas C., van Tendeloo G., van Landuyt J., Amelinckx S.: J. *Solid State Chem.* **84**, 314 (1990).
33. Unkelbach K.H., Becker Ch., Köhler H., von Middendorff: Phys. Status Solidi **B60**, K41 (1973).
34. Horák J., Lošťák P., Geurts J.: Phys. Status Solidi **B 167**, 459 (1991).
35. Novotný R., Zweck J., Starý Z., Navrátil J.: will be published
36. Horák J., Navrátil J., Starý Z.: J. Phys. Chem. Solids **53(8)**, 1067 (1992).
37. Miller G.R., Che-Yu Li J.: J. Phys. Chem. Solids **26**, 177 (1965).
38. Horák J., Novotný R., Lošťák P., Höschl P.: J. Phys. Chem. Solids **48**, 1227 (1987).
39. Horák J., Starý Z., Matyáš M.: J. Solid St. Chem. **93** , 485 (1991).
40. Yim V.M., Rosi F.D.: Solid-State Electronics, **15**, 1121 (1972).
41. Starý Z., Novotný R., Horák J., Navrátil J.: J. Mat. Sci. Letters **12**, 359 (1993).
42. Lošťák P., Horák J., Novotný R., Klikorka J.: J. Mat. Sci. Letters **6**, 1469 (1987).
43. Ionescu R., Jaklovszky J., Nistor N., Chiculita A.: Phys. Status Solidi **A27**, 27 (1975).
44. Starý Z., Navrátil J., Plecháček T.: *Proceedings of 13th International Conference on Thermoelectricity, Kansas City*, 286 (1994)